MEASUREMENT AND NUMERICAL SIMULATION OF MOISTURE TRANSPORT BY CAPILLARITY, GRAVITY AND DIFFUSION IN POROUS POTASH BEDS

A Thesis

Submitted to the College of Graduate Students and Research

in Partial Fulfillment of the Requirement for the Degree of

Master of Science

in the Department of Mechanical Engineering

University of Saskatchewan

By

Ru Gang CHEN

Saskatoon, Saskatchewan

PERMISSION TO USE

The author grants permission to the University of Saskatchewan Libraries to make this thesis available for inspection. Copying of this thesis, in whole or in part, for scholarly purposes may be granted by my supervisors (Prof. Robert W. Besant and Prof. Richard W. Evitts), the head of the Department of Mechanical Engineering, or the Dean of the College of Engineering. It is understood that any copying or publication or use of this thesis or parts thereof for financial gain shall not be allowed without my written permission. It is also understood that due recognition to me and the University of Saskatchewan must be granted in any scholarly use which may be made of any material in this thesis.

Requests for permission to copy or to make other use of the material in this thesis in whole or in part should be addressed to:

Head, Department of Mechanical Engineering

University of Saskatchewan

57 Campus Drive

Saskatoon, SK

Canada

S7N, 5A9

ABSTRACT

As a hygroscopic salt, granular potash can easily absorb large quantities of water vapor from humid air during storage and transportation processes. Subsequent drying will result in potash particles sticking together to form clumps or cakes. In order to avoid or decrease caking, it is essential to know the local history of moisture content and moisture movement in a bed of potash. In this thesis, experimental measurements and numerical simulations are used to investigate moisture transport and redistribution by capillarity, gravity and diffusion effects within a potash bed.

The important properties required to model moisture transfer in granular porous potash (i.e. porosity, permeability, specific surface area and irreducible saturation) are investigated experimentally and theoretically. It is shown that for a mixture with a wide range of particle sizes the potash bed properties can be predicted knowing the properties for each narrow range of particle size in the mixture.

An experimental test facility was designed and constructed to test moisture transfer within a potash bed. The test procedures are presented along with an uncertainty analysis. The moisture content spatial distribution for different particle sizes under different initial conditions is investigated and data are presented.

A one-dimensional transient numerical model of moisture transport accounting for diffusion, capillarity and gravity effects within potash beds is developed. Two

different moisture transport mechanisms are presented. In a wet region, where local moisture saturation level, S, is larger than an irreducible saturation, S_0, liquid water exists as continuous liquid film on the particles; moisture is transferred by liquid film movement due to capillarity and gravity effects. In a dry region where S is less than S_0, water vapor diffusion is the only mechanism of moisture transfer and water is adsorbed in layers on the surfaces.

From the experimental data and numerical simulation analysis, it is shown that the irreducible saturation, S_0, is a strong function of particle size. It will decrease with a particle size increase.

The numerical model is validated by comparison with some typical experimental case studies. Agreement between the experimental data and simulation results is well within the experimental 95% uncertainty bounds. It is concluded from this research that the complex moisture transport process by diffusion, capillarity and gravity effects within a potash bed can be modeled and simulated. Experimental and simulation results indicate that direct water drainage will more readily occur for large particle sizes than for small particles for the same initial moisture content.

ACKNOWLEDGEMENTS

I would like to firstly express my sincere and deepest appreciation to my supervisor Prof. R.W. Besant for his encouragement, patience, guidance and expertise in every stage of my graduate study. Without his support, I could not complete my MSc program in Canada. His academic and moral support is deeply appreciated. His knowledge, kindness, thoughtful insights and vision have provided me with lifetime of benefits. My sincere thanks also extends to my co-supervisor Prof. R.W. Evitts, who provided lots of advice and impetus for this project, and gave his patience and expert guidance throughout my study.

I am grateful to my advisory committee members: Prof. D.A. Torvi and Prof. C. Simonson for their valuable comments and suggestions on the thesis draft improvement. Thanks to Mr. Dave Deutscher and Mr. Darren Braun to provide technology assistance and help for the experimental studies. Thanks also go to Dr. Hong Chen, who worked with me in the same research group. I really appreciate his assistance and truly interesting and versatile discussions, research related or not.

The most grateful thanks are extended to my parents and parents-in-law for their supports and helps during the entire period of graduate study.

Special thanks are given to my wife for her everlasting love, encouragement and support.

Financial assistance from the Natural Science and Engineering Research Council of Canada (NSERC) and the Potash Corporation of Saskatchewan (PCS) is also acknowledged and appreciated.

DEDICATION

This thesis is dedicated to my wife Dan Pu

CONTENTS

List of Tables

List of Figures

Nomenclature

A	test container cross-section area	(m^2)
A_0	surface area of particles divided by the volume of the bed	(m^{-1})
A_{0e}	equivalent A_0	(m^{-1})
A_{sf}	solid-fluid interface surface area	(m^2)
A_S	specific surface area of potash per unit mass	(m^2/kg)
$A_{S(V)}$	specific surface area of potash per unit volume	(m^2/m^3)
d_e	equivalent particle diameter	(m)
d_h	hydraulic diameter	(m)
d_i	diameter of particle size (i=1~4)	(m)
d_j	diameter of particle size (j=1~4)	(m)
d_p	particle diameter	(m)
$\overline{d}_p$	average particle size	(m)
d_{pi}	particle diameter of ith size range of particle	(m)
D	the binary diffusion coefficient for water vapor in air D=0.26E-4	(m^2/s)
D_{eff}	effective diffusion coefficient	(m^2/s)
D_p	particle diameter after considering particle shape	(m)
g	acceleration due to gravity	9.8(m^2/s)
h	equivalent static liquid depth	(m)
h_0	reference static liquid depth	(m)
J	water molecular diffusive flux	(kg/m^2s)

k_k	Carman Kozeny constant	
K	permeability	(m^2)
K_m	permeability of mixture	(m^2)
K_0	empirical coefficient: K_0=2.5 for shaken, K_0=4.0 for unshaken	
K_β^0	permeability for saturated flow	(m^2)
$\dot{m}$	moisture accumulation rate	(kg/m^3s)
MC	moisture content (w/w)	
n	empirical parameter in Eq. (4-3)	
N_{Bo}	Bond number	
p_i	packing fraction for i^{th} component	
p_i^T	calculated packing fraction for i^{th} component	
p_{ij}	packing fraction of i, j component mixture	
p_m	packing fraction of mixture	
P	pressure	(Pa)
P_v	vapor pressure	(Pa)
P_{vsat}	saturation vapor pressure	(Pa)
Q	volume flow rate	(m^3/s)
r_{ij}	ratio of diameters of particles iand j	
R_v	gas constant	(J/kg.K)
Re_d	Reynolds number $= \frac{ud_p}{\upsilon}$	
RH	relative humidity	
S	saturation	(m^3/m^3)

S_0	irreducible saturation	(m^3/m^3)
S_{0m}	irreducible saturation of mixture	
Sl_0	empirical parameter for determining moisture transfer through interface	m^{-1}
T	temperature of potash bed	(K)
t	time	(s)
U	95% uncertainty	
u_D	Darcy velocity	(m/s)
X_i	fraction of solid volume	
X_{ij}	fraction of solid volume for binary mixture i and j component	

Greek Symbols

ε	porosity	
ε_m	porosity of mixture	
ε_σ	volume fraction of the dry granular potash bed	
ε_β	volume fraction of water in the potash bed	
$\varepsilon\gamma$	volume fraction of vaporr in the potash bed	
ρ_a	density of air	(kg/m^3)
ρ_B	bulk density of potash	(kg/m^3)
ρ_β	density of water	(kg/m^3)
ρ_s	density of pure solid potash	(kg/m^3)
ρ_v	density of vapor	(kg/m^3)
τ	tortuosity of particle bed	

μ	air viscosity (21°C) 18.1×10^{-6}	(Pa·s)
η_β	viscosity of water-salt solution in the potash bed	(Pa·s)
ω	moisture content based on mass fraction	
ω_0	irreducible moisture content	
ω_e	the equilibrium moisture content	
ω_m	empirical constant	
ϕ	relative humidity of air	
σ	surface tension	(N/m)
ΔX	height of potash sample	(m)

Others

$<P_c>$	volume average pore or capillary pressure	(Pa)

CHAPTER 1

INTRODUCTION

1.1 Introduction

With increasing world population, human beings have to consider how to sustain the demand for food. It was predicted by Malthus (1798) that the earth could not afford a human population in excess of 4 billion. To feed the increasing world population, even as late as the early decades of the 20th Century, people used the approach that continually enlarges cultivated areas to satisfy the requirements for food. However, the area of cultivated land could not be increased indefinitely. When wetlands that help maintain the earth's ecological balance were cultivated, adverse impacts on the environment resulted. Methods for improving crop production were sought to satisfy the nutritional requirements of the expanding population. Improved plant selections, better soil management and the use of fertilizers became important to improve crop yields. Widespread availability of all kind of natural and synthetic fertilizers has fuelled the agricultural revolution. Correspondingly, research all on fertilizers from their production, handling and storage to application is ongoing.

Fertilizer is a substance applied to soil to enhance its ability to produce plentiful, healthy plants. It can greatly increase the fertility of soils. Nitrogen, phosphorus and potassium are three of the most important nutrient elements for plant growth. In modern

intensive agriculture, the natural supply of nitrogen, phosphorus and potassium from soils is usually not adequate to sustain high yields. For this reason, soil supplies have to be supplemented by fertilization, which increases the amount of these essential elements readily available for uptake by plants.

As one of the most important potassium fertilizers, potash is widely used around the world. The use of potash fertilizer has increased rapidly over the past 40 years and global consumption increased from 8.48 million tonnes in 1960-1961 to 22.15 million tonnes in 2000-2001. (http://www.fertilizer.org/ifa/statistics.asp International Fertilizer Industry Association, 2002). It is mined from potash ore or deposits, which are often 1000 meters underground. Some potash is also obtained from brines and such saline waters as those of the Dead Sea and Great Salt Lake by natural evaporation in solar ponds. After it is produced and processed in a solution or flotation process, the final products are available in different types, each with different size distributions. These types include granular, standard and soluble. Figure 1-1 shows samples of potash produced by a flotation process where the color in the top three samples is caused by the presence of trace amounts of iron oxide, while the bottom three samples are produced in a solution process. Usually the particle sizes range from 0.05 to 5.0 mm diameter, but most products sold have a narrow range of sizes to reduce the handling problems.

The main chemical component of potash is composed of potassium chloride (e.g. more than 98%) or sylvite (KCl) and a small fraction of sodium chloride or halite (NaCl) and carnallite ($KMgCl_3 \cdot 6H_2O$). These salts are hygroscopic with deliquescent relative

humidity of about 52% for carnallite, 75% for halite and 85% for sylvite. At high ambient air relative humidities, potash is especially susceptible to attack by airborne moisture. After exposure to water, solid, liquid and gas phases can exist simultaneously in a potash bed. Figure1-2 shows a schematic of these three phases in a small element of a potash bed. For small particles of potash without any internal water, water will be adsorbed on each surface. Water can exist in a mobile liquid solution on the particle surfaces and it can saturate the interstitial air at or near the air-liquid interface.

Figure 1-1: Samples of potash

When local ambient air relative humidity exceeds 50%, potash readily absorbs large quantities of water vapour from air during storage and transportation processes. As water is adsorbed, some salts are dissolved on the particle surfaces. Subsequently, when the

relatively humidity drops, moisture will be removed from particles by a drying process leaving crystals of KCl, NaCl and $KMgCl_3 \cdot 6H_2O$ in a different location, due to brine migration, in the potash bed. Under small pressures due to the weight of the particles above, crystal bridges may form between particles so that particles are bonded together to form big chunks or clumps. Other small deposited particles remain unattached and form dusts when potash is moved. Caked potash with strong inter-particle bonds cannot be uniformly distributed by most agricultural machines so agricultural plants either receive too much caked potash fertilizer or perhaps none at all.

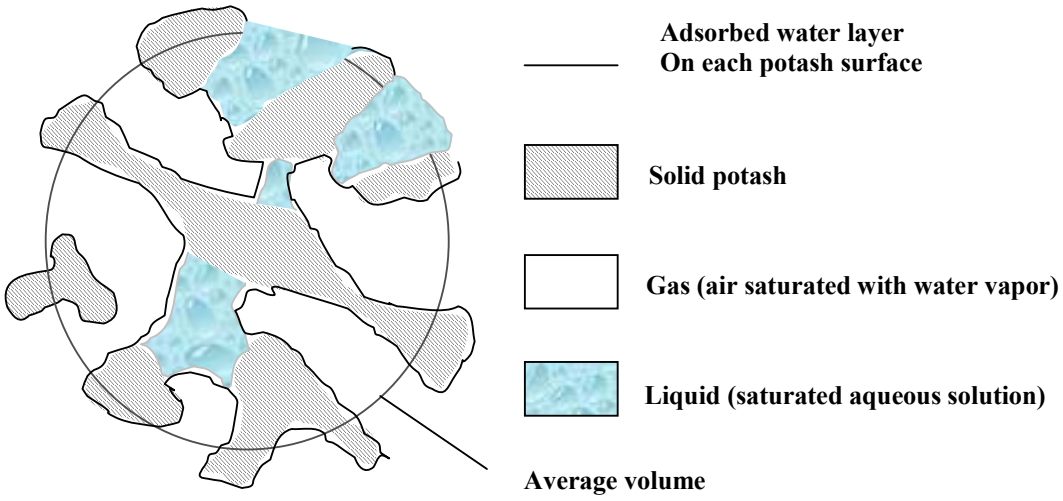

Figure 1-2: Three phases present in hygroscopic potash

The Potash Corporation of Saskatchewan (PCS) is the largest producer and leading exporter of potash in the world. PCS accounts for more than 33 percent of world production. Every year, millions of tons of potash fertilizer products are exported to the United States, Brazil, China, Australia and other overseas markets. Before potash is eventually spread to the soil, potash usually undergoes a two or three month storage

process in warehouse or shed that has no temperature and humidity control. During storage and transportation, potash may experience temperature and humidity changes. Moisture accumulation on the potash surface will penetrate and transfer toward the inside of potash bed over time. For this reason, large quantities of potash are wasted due to serious caking. Understanding the mechanism of caking and studying the transfer of moisture in potash beds to devise practical means of preventing caking thus has economic benefits.

1.2 Factors Related to Caking of Potash

Caking in potash is a very complex process. The nature of caking is the growth of crystal bridges between potash particles at or near contact points between particles in a bed. These crystal bridges develop during storage and transportation due to continuous internal water interactions and thermal effects that result in deposition of crystals under certain conditions from the salt solutions present in the potash bed. There are many factors that influence the rate and extent of potash caking, including chemical composition; particle size and packing; moisture content; ambient air humidity; hydrostatic pressure; and temperature.

(1) Chemical composition and hygroscopicity

The inherent hygroscopic properties of the salts in typical potash particles are the most direct reason for caking. Particles with different chemical composition have

different moisture adsorption properties such that particles with high concentrations of carnallite and halite will adsorb more water at lower relative humidities. Pure sylvite will only adsorb large fractions of water when the ambient air relative humidity is greater than 84%. Anti-caking and anti-dusting agents are often used to reduce caking when potash anti-caking agents are added to alter the surface tension of the aqueous films on the potash particles.

(2) Particle size and packing

Potash particles come in a wide range of sizes from a fine dust (e.g. 10μm) to about 5mm in diameter. Since the surface area of these particles is proportional to the square of the diameter while the volume varies with the cube of diameters, the specific area per unit volume will be 500 times greater for the smallest particle compared to the largest particle. Furthermore, for equal thicknesses of moisture adsorption layers on the surfaces of each particle a bed of the smallest particles will have a moisture content 500 times larger than a bed of the largest particles. Conversely, for equal moisture content the moisture adsorption layers on the smallest particles will be 500 times thinner than the largest particles.

The number of contact points between particles in a bed depends on the distribution of particle sizes in the bed and the amount of vibration experienced by the bed prior to a test. Generally, the wider the range of particle sizes, the tighter the packing the smaller the void fraction or porosity. As well, the porosity is also reduced by typically

10% after a bed is vibrated from an initial fill condition. The number of contact points between particles in a bed depends on both these factors so that there may be a few as 4 contact points or as many as 10 per particle. Again, since small particles have a large specific surface a bed of the smallest particles will have 500 times the number of contact points per unit volume of bed compared to the largest particles.

(3) Moisture content

The moisture content is an essential factor if caking is to occur. If there is no moisture content in potash, no caking occurs. Caking only occurs at a condition where there is a certain moisture content (e.g. above 0.25%) followed by a subsequent drying process. The amount of moisture allowed remaining in finished potash fertilizer should always be less than 0.25% and preferably even lower because some moisture will likely be gained during shipping and storage.

(4) Relative humidity of the adjacent air

Caking is closely related to relative humidity variation of the adjacent air. The difference between relative humidity of the air and the critical relative humidity of potash will greatly influence the adsorption rate of moisture. When a dry potash sample is exposed to humid air with relative humidity lower than the critical relative humidity of 52% (carnallite), the potash will adsorb some water vapour by Van der Waals forces and a monolayer of adsorbed water on each surface may exist. The corresponding equilibrium

moisture content is very small. When the relative humidity exceeds the critical relative humidity, the chemical potential (partial Gibbs free energy) of water vapour in humid air is higher than that of water in the surface aqueous solution, and the water vapour will condense continuously until a new equilibrium is reached. During storage and transport the potash may experience a wide change in air relative humidity conditions due to environmental temperature fluctuations. Figure 1-3 shows typical data of one indoor and one outdoor temperature and relative humidity sensor inside and outside of a potash storage shed in Vancouver, B.C. These data, during a high outdoor ambient air relative humidity period of 26 days, show an interior humidity above 50% except for a few hours on the day 23. It is expected that water vapour would be transferred from the air to the potash during most if not all of the days.

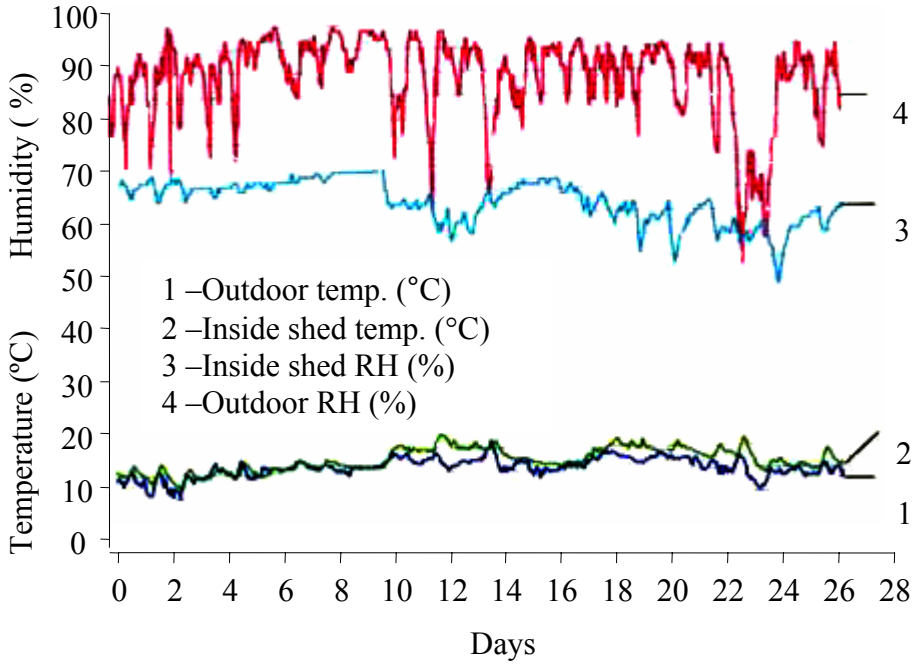

Figure 1-3: A typical change of temperatures and relative humidities of indoor and outdoor potash storage shed (January 1999, at the Canpotex Neptune terminals, Vancouver, B.C. Canada)

(5) Pressure in potash pile

Hydrostatic pressure is a necessary factor for caking. The degree of caking is dependent on the storage static pressure due to the mass of particles above each point. The increase of pressure means that the contact points between particles increase, which induces particles to cake more easily. Pressure can be controlled by limiting the height of bulk storage piles.

(6) Temperature

Temperature is also another important factor in the caking process. The moisture accumulation and transfer in potash beds is generally closely coupled with heat transfer and temperature distribution as well as environmental air properties such as air temperature, air relative humidity and air flow velocity. The heat released by adsorption, condensation and dissolution will change the temperature of both the potash particles and the air within the pores of potash particle beds. If the potash beds undergo high temperature or water vapour variations, potash beds tend to cake more seriously after water evaporation and the growth of crystal bridges.

In this study, accurate measurements are to be performed and models of moisture content transfer developed to predict the redistribution of moisture within a potash particle bed. Special emphasis is given to measurement accuracy and modeling moisture

migration in potash beds. Different particle size ranges are tested and modeled when capillarity, gravity and vapour diffusion effects of water occur.

1.3 Literature Review

1.3.1 Moisture Accumulation and Transfer Research in Potash

Since the 1930's many papers and reports have been published concerning the handling, caking and application of fertilizer products such as potash. But only a few have been published that are directly concerned with moisture content and transfer in potash fertilizer. In recent years, more attention has been given to avoiding caking in the fertilizer industry due to the extra transport and handling costs. Recently, some papers that have developed theoretical models of adsorption and the dissolution process in potash and others that have measured and analyzed heat and mass transfer in a granular potash bed.

Thompson (1972) presented a comprehensive review of caking in typical granular fertilizer products. His research results revealed that important factors such as moisture content, pressure, temperature, time to expose in humidity environment are closely related to the caking of granular fertilizers stored in plastic bags. He concluded that crystal bridging is not a major cause of caking and stress is essential because it alters the solubility of salts and the pore pressure of thin aqueous films.

Pyne et al. (1996) studied the interaction between water vapour and granular potash fertilizers. In their research, the rate of water vapour uptake by potash as a function of water vapour pressure over a potash sample was measured by using an isothermal heat conduction calorimeter. Results showed that there are transitions during the moisture uptake process, one occurring at about 0.60 RH where significant moisture accumulations begin, and the other at about 0.84 RH.

Hansen et al. (1998) investigated the effects of anticaking agents on the thermodynamics and kinetics of water sorption by potash fertilizers using the same calorimetric method as Pyne. Enthalpy changes for water sorption were estimated from the temperature dependence of equilibrium vapour pressures. This research stated that anticaking agents apparently help to prevent cementitious crystals from growing between particles either by preventing contact of surface solution films or by modifying the crystal morphology of the cementitious layers, instead of by slowing or diminishing the sorption of water.

Walker et al. (1998) were engaged in the caking research of mixed granular nitrogen, phosphorus and potassium (NPK) fertilizers. Their research indicated that caking process is dominated by free water accumulation and movement through capillary adhesion and a crystal bridging process. It was concluded from this investigation that the accumulation and movement of free water is interlinked with the caking process. Capillary adhesion forces between granular particles are increased by high concentrations

of free water in that it causes the granules to be more pliable, which increases the contact area and surface tension capillary effects between granular particles.

In recent years, a series of research works concerned with heat and moisture transfer in potash have been performed at the University of Saskatchewan. Peng et al. (1999) presented the solubility analysis of potash fertilizer at thermodynamic equilibrium. The thermodynamic equilibrium constant method was used to analyze and solve the equilibrium dissolution reaction of potash with moisture as a function of the adjacent air relative humidity or surface solution activity. A critical relative humidity around 52% with slight temperature dependence was found for the transition from adsorption to dissolution and the onset of condensation on potash as the consequence of the existence of small fraction carnallite on the particle surfaces. The moisture-potash interaction mechanism as adsorption or condensation was characterized. A small fraction of moisture by adsorption will be picked up once the environmental relative humidity is lower than 52%. When relative humidity exceeds 52%, water vapour will condense and cause dissolution of potash until a new equilibrium is reached. The relationship between the relative humidity and the equilibrium moisture content was established by the dissolution equilibrium calculation.

Further, Peng et al. (2000) experimentally and numerically studied the heat and mass transfer in granular potash fertilizer with air flow through a potash bed. A one dimensional experiment was set up to measure the temperature and outlet air humidity response and mass gain of a potash bed subjected to a step change in air flow. The

transient temperature and moisture content distribution was predicted using a porous media mathematical model and numerical simulation. Experimental and numerical results showed that non-equilibrium internal moisture and heat transfer processes existed in the bed with significant differences in pore air and particle temperatures and surface water activity and pore air relative humidity. Results showed that the dissolution of potash due to humid air flow through potash bed causes a significant temperature rise and humidity decrease in the exhaust air. The dissolution heat source in potash-water vapour interaction causes the temperature of solid particles to be higher than air temperature during the transient adsorption process, necessitating the use of two coupled energy equations for the bulk gaseous and solid-liquid subsystems.

Arinze et al. (2000) collected experimental test data on thin-layer moisture adsorption and drying for different potash products. Analysis of experimental data shows that there are significant differences in the moisture adsorption characteristics of different potash fertilizer products. They found that (1) the rate of drying of a potash product increases as the air humidity decreases or as the temperatures increases, and (2) drying air temperatures have a more important effect on the rate of drying than the air humidity. Based on the experimental data, thin-layer moisture adsorption and drying models were developed to simulate moisture uptake and drying in normal potash storage piles under different environment conditions. In another study, Arinze et al. (2001) investigated the effects of material and environmental conditions on caking and breakage of potash fertilizer products during storage, shipping and handling from several points of view such as combined effect of moisture, time and pressure on caking, and the effect of pressure on

product breakage and dust formation. The newly developed mathematical models may be useful in predicting potash product quality.

Zhou (2000) studied the moisture accumulation on the surface of granular potash fertilizer products. The coupled heat and moisture transfer during the handling process and warehouse storage was modeled as a one-dimensional transient heat and moisture diffusion problem at the air-potash interface. This one-dimensional transient numerical model of heat and moisture transfer, including adsorption/dissolution and condensation, was compared to measured data. Relevant temperature and moisture content profiles were measured in the potash bed subject to one-dimensional heat and moisture diffusion. The simulation results were compared with measured data under a wide range of test conditions for two types of potash.

Gao (2001) considered the use of a dry air wall jet to protect potash from humid air in large storage buildings. In this research, an experimental test facility was designed to investigate wall jet mean velocity, relative humidity and moisture accumulation at the potash-air interface. Several characteristics of the wall jet such as the decay of the maximum velocity; the growth of the jet half-width; the self-similarity of the wall jet with distance from the jet exit; and the skin friction coefficients and mass transfer coefficient were systematically observed and analyzed for the fully developed flow region of the wall jet. Both rough and smooth surfaces were studied. Experimental results and numerical analysis with corresponding uncertainty show that the maximum velocity decays much more rapidly for a rough surface than for a smooth surface. The skin friction

coefficients were obtained from log-law velocity correlations and skin friction coefficient. This research shows that a wall jet of dry air may be used to reduce moisture adsorption by potash.

Faraji et al. (2002) use near infrared (NIR) spectroscopy to investigate the correlations between moisture content and spectral reflectance for red standard potash within a range of moisture content from 0% to 6%. The research investigated some reflectance properties of red standard potash in the visible and infrared portions of the electromagnetic spectrum and developed a correlation model for moisture content as a function of reflectance at selected wavelengths. This technology could lead to the development of remote sensing on-leave is on the surface of in potash piles or on-line process moisture measurement.

Although these documents provide much valuable information, they mainly concentrate on the moisture adsorption and some anti-caking and remote sensing investigations. They only take account of the diffusion effect of water vapour transfer, with no consideration for moisture movement by capillarity and gravity even though it appeared to occur in some of the test data. Often moisture transfer in potash is greatly influenced by capillarity and gravity effects because, when it occurs, it is usually orders of magnitude larger than the vapour diffusion mass flux. Moisture transfer by capillarity and gravity as well as vapour diffusion should be considered experimentally and in a theoretical/numerical model.

1.3.2 Moisture or Water Transport in Porous Media

The problem of multiphase flow and transport (water and water vapour) in porous hygroscopic materials is one of long-standing interest and is of increasing importance. Although this problem has been studied from both experimental and theoretical perspectives since the beginning of 20th Century, many researches still focus their attention in these fields. Some research papers concerned with moisture or water transport within porous media such as soil, food products or textiles and building materials have been published. For simple problems with no capillarity and gravity effects both the experiments and theoretical/numerical equations for water vapour diffusion are simpler. Whitaker (1977) presented a set of equations that consider heat and mass transfer due to temperature difference and moisture movement for porous media that remains invariant in the solid phase for any process. This rigorous theoretical approach to the problem of drying granular porous media gave very good agreement with measured data when capillarity does not occur. In 1980, Whitaker focused on understanding the properties of moisture transport in porous media when the effects of capillarity and gravity dominate. Although there is some experimental data to compare with this model for water movement in a sand bed, there appears to be no data for salts such as potash.

Puiggali et al. (1988) examined the influence of gravity on the moisture transport process during the isenthalpic drying period. Vapour diffusion models were used to predict both saturation profiles and to extract apparent diffusivities from experimental

data. For granular or unconsolidated porous media, the one-dimensional moisture transport process were be characterized by two dimensionless groups that accounted for capillary forces, gravitational forces and viscous forces. Numerical simulation results of the saturation transport equation indicated the circumstances that the diffusion model can be used and under what circumstances the diffusion model can be used to predict saturation profiles even though it is an incorrect representation of the moisture transport process.

Ghali et al. (1994) developed a conservation equation for moisture transfer in fabric as a function of capillary pressure and permeability under isothermal conditions. The equation includes the transfer of both liquid by capillarity and vapour by diffusion in the fibrous medium. This equation was solved numerically by finite-element method and was applied to two different samples. Results show that this model is capable of simulating the wicking process including the effect of gravity on moisture transport.

Kolhapure et al. (1997) studied an unsaturated flow of moisture in porous hygroscopic media at low moisture contents. A mathematical description of thermal drying process involving various mechanisms of moisture migration such as water sorption, diffusion and solid-moisture interactions in hygroscopic materials was developed for unsaturated flow region. The moisture transport model was derived for the drying of porous hygroscopic solids and was formulated using microscopic mass balance and volume averaging techniques. The model accounts for the solid-moisture interactions through wettability potential by modifying the constitutional Darcy's law. The wettability

potential was defined in terms of water activity and was incorporated with Darcy's law. The effective diffusion coefficient was given by the sum of the liquid and vapour diffusion coefficients.

1.4 Research objective:

Reviewing the literature on moisture accumulation and transfer in fertilizer and capillarity, gravity and diffusion research in porous media, indicates that no research has been published in which a numerical model is developed to predict moisture transfer in potash beds where capillarity and gravity effects are important. However, it is also important to know the actual moisture content distribution for a given potash bed under certain conditions. Based on different potash particle size distributions, the inherent properties and different initial conditions, accurate measurement of moisture content distribution within a potash bed and numerical model simulation/prediction for moisture content within a potash bed after certain storage duration is of great practical significance. This model which sufficiently considers the actual physical transport process of moisture will hopefully provide prediction for moisture distribution within potash storage under different environmental conditions such as humidity. The objectives established for this study are:

(1) To experimentally and theoretically investigate the properties required to model moisture transfer in granular porous potash by capillarity, gravity and diffusion within a particle bed. These properties are porosity, permeability, and specific surface area.

(2) To design and construct an experimental apparatus to test moisture transfer within a potash bed, and to analyze and specify the uncertainty for each experiment.

(3) To develop an appropriate numerical model for water accumulation and redistribution within a potash bed that includes all significant physical effects such as diffusion, capillarity and gravity, for a one-dimensional moisture transfer processes.

(4) To validate the numerical model by using measurement data of moisture distribution with specified uncertainty.

(5) To investigate the moisture transfer process for typical operating conditions in potash beds through case studies.

In order to achieve the objectives mentioned above, research steps were implemented to measure the potash properties, moisture distribution and to develop a theoretical model. These steps include:

(1) Measure the essential properties of granular potash fertilizer required for modeling. These include bed porosity, permeability and specific surface area, for narrow particle size ranges. Perform an uncertainty analysis on these data. Develop a method to predict these properties for a mixture with wide range of particle sizes after knowing the properties of each narrow range of particle sizes.

(2) Develop and construct a one-dimensional potash bed test facility for a moisture transfer study. Determine the initial and final moisture content distribution for different initial condition combinations and different potash particle size distributions.

(3) Determine irreducible saturation for different particle sizes. This is the key parameter of the moisture transport model.

(4) Compare the measured data and numerical simulations for each test and analyze the uncertainty and discrepancy between the results.

1.5 Overview of Thesis

The presentation of this research begins in Chapter 2 with a detailed description of the test facility, including instrumentation and measurement techniques for the determination of porosity, permeability and specific surface area for narrow size ranges of particles. A method to predict porosity of a mixture with wide range of particle size is also presented in this chapter.

Chapter 3 presents the experimental apparatus to measure moisture content distribution within a potash bed by diffusion, capillarity and gravity for a specific transfer time. A wide range of initial moisture content conditions are produced in the laboratory to study the irreducible saturation for different particle sizes. Detailed test procedures and uncertainty analysis for each test procedure are described.

Chapter 4 develops a mathematical/theoretical model of moisture accumulation and redistribution in a potash bed that accounts for complex physical phenomena such as diffusion, capillarity and gravity effects.

Chapter 5 shows the validation and prediction of the model by comparing numerical calculations and measured experimental data. The relationship between irreducible saturation and particle size is revealed.

In Chapter 6, the summary and conclusions of this research are presented. Several recommendations and suggestions for future work are proposed.

The Appendices include: (A) Uncertainty analysis for porosity, permeability and specific surface area. (B) Control volume formulation for discretization of governing equations and boundary conditions. (C) A detailed numerical algorithm for simulating moisture transport within potash bed is presented. (D) Properties used in the numerical model. (E) Moisture transfer experimental data.

CHAPTER 2

DETERMINATION OF POROSITY, PERMEABILITY AND SPECIFIC SURFACE AREA PROPERTIES

2.1 Introduction

The use of experimentally validated numerical models for studying moisture transfer behaviour in porous media has become common practice because the experiments required are complex and time consuming. In order to accurately model moisture accumulation and movement within a porous media and obtain reliable simulations, characterization of material properties is essential. Potash is a solid material comprised of irregular crystalline particles. The macroscopic properties of a potash bed are influenced by the pore structure of the bed because this void space provides the conduits for transporting liquids (i.e. water) or gases (i.e. air or water vapour). An exact description of the medium, based on structural information on the pore-scale, is unfeasible. Therefore, the structural quantities averaged over a larger volume are defined. The pore space is filled with air and/or water, leading to a multiphase system requiring a mass balance equation for each species and volume balances for each phase. Pore structure parameters are those properties that are completely determined by the pore structure of the medium averaged over many adjacent particles in a bed.

The most important macroscopic pore structure parameters are porosity, permeability and specific surface area. Determining these properties is of practical significance for quantifying the structure and phase composition of porous media and modeling moisture transport within a potash bed by diffusion, capillarity and gravity drainage.

Potash is sold in various particle size ranges from the soluble grade with 95% of the particles in the range ($0.05<d_p<0.3$ mm), standard grade ($0.2<d_p<2.0$ mm), the granular grade ($2.0<d_p<3.96$ mm), and an extra large grade ($3.0<d_p<5.0$ mm). It can be seen from this that there is a large range of particle sizes for each product grade (i.e. typically a variation of particle diameters of a factor of about 2 to 10) and overlapping sizes between some grades. Furthermore, since there is a significant variation in product properties such as porosity, permeability, specific surface area and irreducible saturation with various ranges of product particle sizes, the measurement of these properties for a product with a wide range of particle sizes means that all the properties may change if the distribution of particle sizes shifts for any product grade.

It may be more useful to first investigate these properties using test samples with a narrower range of particle sizes and then combine these properties when various sizes of particles are mixed together to form a product grade. As a first study of granular potash fertilizer products, the emphasis will be placed on the methodology of testing for one product and the accuracy of the data rather than presenting a complete data set of all product grade size ranges. For these reasons, this study is focussed mostly on the granular

grade of product with size ranges from 2.0 to 3.96 mm diameter but there are also some investigations of standard grade particle sizes so that the property investigation of general particle size range (average particle diameter 0.5~5 mm) for common commercial product are performed.

The detailed objectives of these property determinations are as follows:

(1) To present data, experimental test procedures and modelling methodology to accurately measure and calculate porosity, permeability, specific surface area of potash test samples. The granular grade of potash with a particle size range 2.0 to 3.96 mm was used in this research to investigate its properties and the particles were sieved into four size ranges (Table 2-1). These property parameters will be used as input parameters for the numerical model.

(2) To determine the data and the relationship between the properties for the narrow size ranges in (1) and that of a combined sample when various sizes are mixed together to form a typical product type.

2.2 Experimental Procedure

As important macroscopic properties for the study of potash, the porosity, permeability and specific surface of potash were measured using typical methods and results were calculated along with uncertainty in each property for various sizes of potash particles.

2.2.1 Sample Preparation and Characterization

Test samples were selected from Lanigan untreated granular potash produced by Potash Corporation of Saskatchewan, Canada. Lanigan untreated granular potash is a granule grade potash product with size ranges from 2.0mm to 3.96mm diameter and is produced without an anti-caking agent. It is usually stored in a sealed bucket to keep the moisture content less than 0.1% (w/w). In order to obtain test samples with a narrower range of particle sizes, the standard commercial sieve series (standard screen scale, W.S. Tyler Company, USA) was used to sieve the granular potash materials into several size ranges. The sieve mesh sizes used were #5, #6, #7, #8, #10 as shown in Table 2-1.

Table 2-1: Untreated granular potash particle size

Mesh number	5	6	7	8	10
Aperture (mm)	3.96	3.35	2.80	2.36	2.00
Particle size d_p (mm)	Range 1	Range 2	Range 3	Range 4	
	$3.35<d_p<3.96$	$2.80<d_p<3.35$	$2.36<d_p<2.80$	$2.00<d_p<2.36$	

A sieve shaker (RO-TAP, Model-B, C-E Tyler, USA) with an electrical motor driven, shown in Figure 2-1, was used to subdivide the original granular potash product.

Figure 2-1: Sieves and shaker used to subdivide the particles

The shaker vibration frequency (5Hz), time duration (15 Min.), and angular position (7.5º inclined) were first selected to cause good horizontal and vertical shaking. Then, combinations of different sized sieves shown in Table 2-1 were selected to sieve the original granular potash product. The sieve shaker was operated for time duration of about 60 minutes resulting in a particle size distribution that was invariant with time. This procedure was repeated on fresh potash samples to generate a large test sample. Four narrower range particle sizes were obtained by this method.

2.2.2 Apparatus and Measurement Procedure

Porosity

Porosity is defined as the fraction of the bulk volume of a sample that is occupied by pore or void space. Figure 2-2 illustrates this definition of porosity. It is known that the actual shape of potash particles is usually irregular and non spherical and the particle size distribution has a strong effect on porosity. In addition, when the bed is shaken or unshaken, the porosity is different. The measurement of porosity can be achieved by a variety of methods, such as the gas expansion method, optical methods or the density method (Dullien, 1992). All these methods aim to measure the void volume and the bulk volume of the material; the ratio of the two values is then the porosity. In this thesis, the density method was used because it gives the most accurate results as it is the most direct method to determine porosity. The following equation can be used to calculate the porosity.

$$\varepsilon\rho_a + (1-\varepsilon)\rho_s = \rho_B \tag{2-1}$$

As the density of air, ρ_a=1.2 kg/m^3**,** is much smaller than the both bulk density of the sample, ρ_B, and the density of the pure solid, ρ_s, the density of air, ρ_a, can be neglected. Therefore, the porosity, ε, is determined by

$$\varepsilon = 1 - \frac{\rho_B}{\rho_s} \tag{2-2}$$

The density method depends on determining the bulk density of sample ρ_B, and the density of the pure solid, ρ_s. The bulk density ρ_B can be easily obtained by weighing the mass of a sample with a certain volume. The density of the pure solid, ρ_s, can be obtained by crushing the solid, weighing and then determining the volume of the particles by measuring the displacement method of oil caused when these particles are immersed

in oil. In this thesis, the density of the pure solid, $\rho_{s,}$ is taken to be 1987 kg/m^3 by PCS and this value is thought accurate. No uncertainty is provided, and then the bulk density of the sample, ρ_B, is measured to give the porosity.

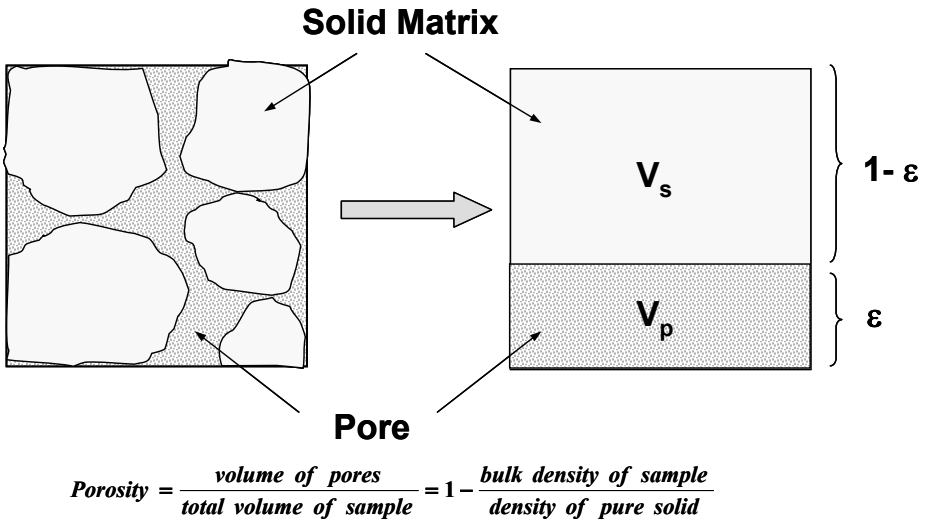

Figure 2-2: Schematic of porosity definition

The experimental setup used to determine the porosity consisted of three main components: the samples, test vessel of known volume, and weigh scale with a high accuracy (±0.001g). Figure 2-3 shows the schematic of this test apparatus. The tests were divided into shaken and unshaken configurations. Firstly, the mass of the empty test vessel of known volume was determined, and then the prepared samples with selected particle sizes were used to fill the test vessel. The vessel is then reweighed.

Figure 2-3: Gravimetric experimental apparatus for porosity measurement

The experimental tests were repeated ten times and the mean value was used as the mean of particles in the vessel. Equation (2-2) was then used to calculated porosity of the particle bed.

Permeability

Permeability, *K*, is the constant of proportionality in the Darcy equation that quantitatively describes the ability of a porous medium to conduct fluid.

The Darcy law holds for flows at low Reynolds numbers (i.e $\mathrm{Re}_{d_p} = u_D d_p / \upsilon < 10$) in which the pressure driving forces are small and balanced only by the viscous forces (Dullien, 1992). Typical value of Reynolds number used in the permeability measurement of standard potash (average particle size 0.8 mm) and granular

potash (maximum average particle size 3.66 mm) were $\mathrm{Re}_{d_p} = 1.26$ and $\mathrm{Re}_{d_p} = 5.75$ respectively. The maximum Darcy velocity in these experiments was 0.022 m/s. Equation (2-3) and (2-4) described the Darcy velocity and these were used to calculated the Darcy velocity.

$$u_D = \frac{K}{\mu} \cdot \frac{\Delta P}{\Delta X} \tag{2-3}$$

The Darcy velocity, u_D, is the total volume flow rate, Q, divided by the flow area, A.

$$u_D = \frac{Q}{A} \tag{2-4}$$

ΔP = pressure drop across the test sample (Pa),

ΔX = depth of sample in the test bed which was 0.15 m for the current tests.

μ = viscosity of air (18.1×10^{-6} kg/m·s)

Measurement of permeability in isotropic media is usually performed using cylindrical containers. The experiment can be arranged so as to have either horizontal or vertical flow parallel to the cylinder axis and through the test sample. Special attention must always be taken to prevent bypassing of the sample by fluid flow adjacent to the wall. This is easily achieved using vertical flow.

In principle, both liquid and gases can be used to measure permeability. However, liquids sometimes change the pore structure and thus permeability due to rearrangement or dissolution of some particles. As potash particle is soluble in aqueous water would not have been used as the working fluid. Hence, dry air was used in the permeability tests. Although, measurement at a single steady flow rate permits calculation of the

permeability from Darcy's law in principle, due to the existence of experimental error in this measurement, several measurements at various low flow rates were used and the results averaged. The measurement of permeability was deduced from measurements of the pressure difference, air temperature and flow rate using the test facility shown in Figure 2-4.

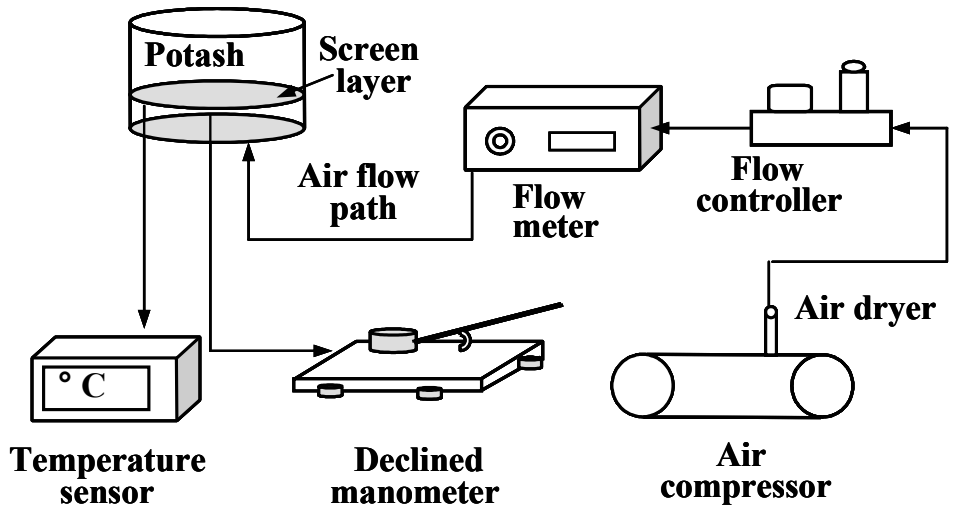

Figure 2-4: Experimental apparatus used to measure permeability

This apparatus is comprised of an air compressor, a large cylindrical test container (I.D. = 306mm) filled with potash, flow-rate controller with a digital LED screen, a temperature sensor with digital LED display, an inclined manometer and a calliper or ruler. A compressor provides dry air at a flow-rate that can be adjusted using the flow-rate controller so that the permeability can be determined at different flow-rates.

The cylindrical test container is shown in Figure 2-5. In order to minimize wall effects and particle alignment effects caused by proximity to the wall, two important

geometric parameters, namely the diameter of the test container (0.306 m) and the depth of test sample (0.15 m), were selected to be about 100 times larger than the particle size (d_p=2.0~3.96 mm). The fibreglass diffuser causes the air supply to be uniformly distributed over the bottom of the particle bed. A screen, with uniform opening size of 800 μm and made of stainless steel, was used to support the test sample.

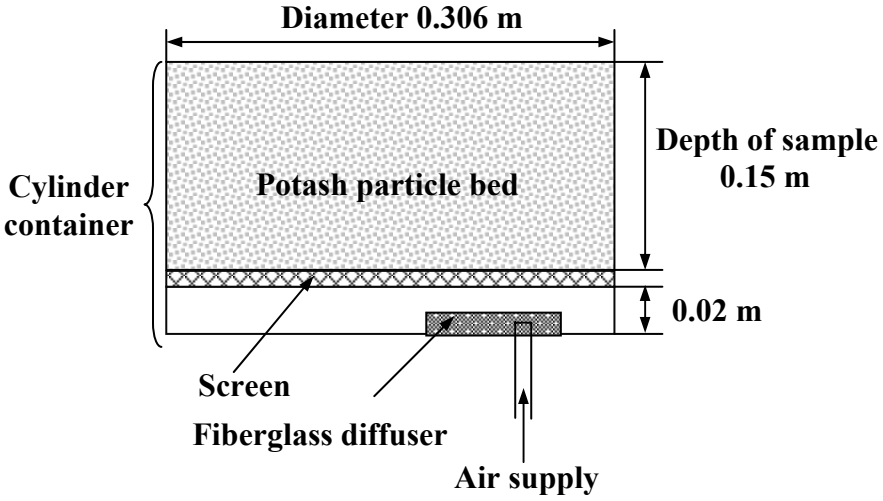

Figure 2-5: Schematic of the test container used in permeability measurement

The test procedure used to measure permeability is as follows:

1) Measure diameter and height of test container.

2) Measure the air temperature.

3) Measure the air flow rate through potash particle bed by using the calibrated volume flow meter.

4) Measure the pressure difference between potash bed and ambient air by using an inclined manometer.

5) Repeat step 3 and step 4 under several different flow rates.

6) Determine viscosity of air in terms of measured air temperature.

7) Calculate the permeability via Equations (2-3) and (2-4).

Specific Surface Area

The specific surface area (A_S) is another important geometric characteristic of porous media. It is the interstitial surface area of the air-solid interface of the particles per unit mass (kg) or per unit volume (m^3) of the porous material. The specific surface of the shaken (consolidated) and unshaken (unconsolidated) granular potash in a bed can be determined using gas adsorption methods or using the correlation equation due to Carman (1938, 1939). In the adsorption method, nitrogen is often used as an adsorption gas which attaches to the surfaces of solids by weak Vander-Waals interactions. This method is not appropriate for potash because the specific surface area is relatively small so there will be a large uncertainty in the measurement.

The Carman correlation (Carman 1938) , is given by:

$$A_S = \left[\frac{1}{k_k \cdot \rho_s^2} \cdot \frac{\varepsilon^3}{(1-\varepsilon)^2} \cdot \frac{1}{K} \right]^{1/2} \quad (\mathrm{m^2/kg}) \qquad (2\text{-}5)$$

For the surface area per unit mass of bed, the specific surface area for shaken and unshaken beds should be same because the particle surface area depends only on the mass. In the current study, the average value of specific surface area, calculated using equation (2-5) as an empirical correlation for shaken and unshaken, is shown in Table 2-

2. The small uncertainty for the average value is weighted by the magnitude of uncertainty for each data point.

The specific surface area per unit volume of bed, $A_{S(V)}$, is then

$$A_{S(V)} = A_S(1-\varepsilon)\rho_s \tag{2-6}$$

where equation (2-2) relates ε, ρ_s *and* ρ_B.

Equation (2-5) is a correlation that depends on the measurement of ρ_s, ε and K, and it also employs a particle shape factor coefficient, k_k, called the Carman-Kozney coefficient. Very good values can be obtained in the literature for this coefficient when the particle shape is nearly spherical (e.g. glass spheres or well rounded sand particles), in which case the uncertainty in specific surface area using the Carman correlation is less than ±20%. For crystalline particles such as potash the value of k_k is not well known and the uncertainty in the Carman correlation will be much greater because this Carman correlation is developed for the nearly round sand particles. For crystalline particles, the shape factor coefficient, k_k, was estimated to be 5 by Carman (1938) based on the fit of experimental data and correlation calculation results. Uncertainty information in the shape factor coefficient was not provided and thus uncertainty in the calculation value of the permeability is not presented here.

2.3 Experimental Results and Analysis

The experimental results for porosity, permeability and specific surface area for several particle size ranges are shown in Table 2-2 for shaken or consolidated and

unshaken or unconsolidated conditions for each test sample. The uncertainty calculations for data in this table are presented in Appendix A.

Table 2-2: Potash properties for different particle sizes and size distribution

Particle size (mm)		Porosity ε	Permeability $K\times10^8$ (m^2)		Specific surface area A_S (m^2/kg)
		Test data	Test data	Calc. Eq.2-20	
$2.00<d_p<2.36$	Shaken	0.412±0.013	1.32±0.07	1.24	0.98±0.20
	Unshaken	0.477±0.007	1.77±0.09	1.78	
$2.36<d_p<2.80$	Shaken	0.406±0.006	1.54±0.07	1.63	0.84±0.17
	Unshaken	0.479±0.004	2.64±0.12	2.55	
$2.80<d_p<3.35$	Shaken	0.410±0.009	2.10±0.06	2.42	0.73±0.15
	Unshaken	0.477±0.004	3.35±0.15	3.56	
$3.35<d_p<3.96$	Shaken	0.400±0.008	2.98±0.12	3.07	0.59±0.12
	Unshaken	0.469±0.010	4.66±0.21	4.63	
Granular product ($2.00<dp<4.00$) $\overline{d}_p = 3.0$	Shaken	0.395±0.013	2.16±0.09	1.82	0.68±0.14
	Unshaken	0.469±0.008	3.47±0.15	2.89	
Equal mix $\frac{1}{2}$ [$(2.00<d_p<2.36)$ +$(3.35<d_p<3.96)$]	Shaken	0.384±0.011	1.49±0.04	1.43	0.79±0.16
	Unshaken	0.458±0.008	2.19±0.06	2.30	

In this table, the uncertainties in each test are presented for the particular sample tested. It was found that different samples from the same bulk sample source for the same size range gave slightly different results and this sample selection uncertainty, associated with different samples from the same source, was about the size of the uncertainty

presented in the table for individual tests. Different bulk sample sources would be expected to increase this sample selection uncertainty because there may be small but significant variations in the product particle size distribution for the same product.

It is evident from these data that the porosity, ε, varies over a small range, 0.400 to 0.412, for the shaken samples for the small range of particle sizes in each of four ranges. The porosity of a sample was found to decrease by about 10% of its initial value if it was shaken or consolidated to its minimum value. This porosity drops slightly for the original sample mix of granular particles and for the equal mix sample. For granular potash, the mass accumulated distribution of particle sizes is shown in Figure 2-6 indicating that it has a range of sieve diameter sizes from 2.0 to 4.0 mm with a mean value of $\overline{d}_p$=3.0 mm. The best fit curve is obtained via the least square method. The computer software Table-Curve (AISN, version 2.01) is used to perform this fit.

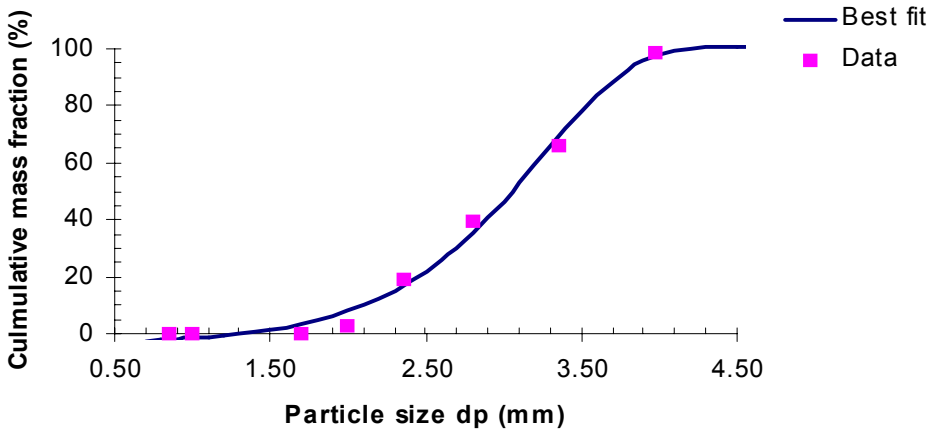

Figure 2-6: Cumulative mass fraction vs. particle size for the original granular product

The unshaken samples were simply produced by pouring each sample into a test container. It was found that the uncertainties in porosity associated with different samples from the same bulk source in the beds for the unshaken state were less than the uncertainties presented for the shaken state. This random variation in porosity sample selection in the shaken state was thought to be mostly due to small packing variations in the filling procedure. That is, the porosity in the shaken state was found to be somewhat dependent on the experimental procedure in filling the test vessel. Furthermore, there will likely be very different shaken property results for very deep beds compared to the very thin beds which were tested (i.e. depths of 0.075 to 0.2 mm in these tests) because compaction tends to increase as the depth of bed increases.

It is will be shown in the next section that the porosity for the original sample mix of granular particles and an equal mix sample for both shaken and unshaken state depends on the size ratio of the particles making up the mix. As illustrated in Figure 2-7, the porosity variation is due to the geometric interactive effects of different sizes of particles, where the small particles fill the voids created by the large particles, results in a smaller porosity for mixed sizes of particles than similar beds with uniform sizes as illustrated in Figure 2-8.

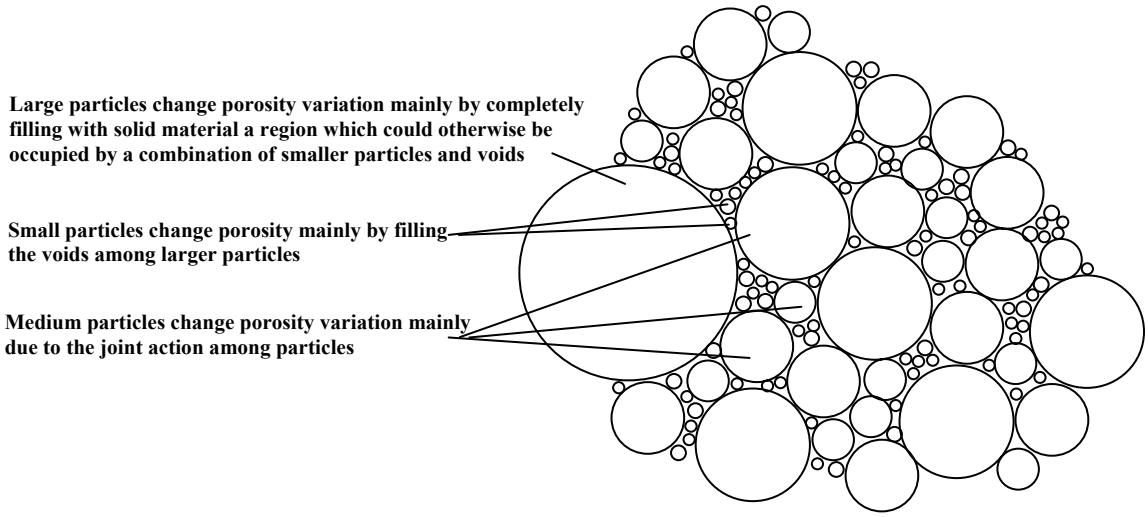

Figure 2-7: Schematic illustrating the space filling effect of spherical particles with a range of particle sizes.

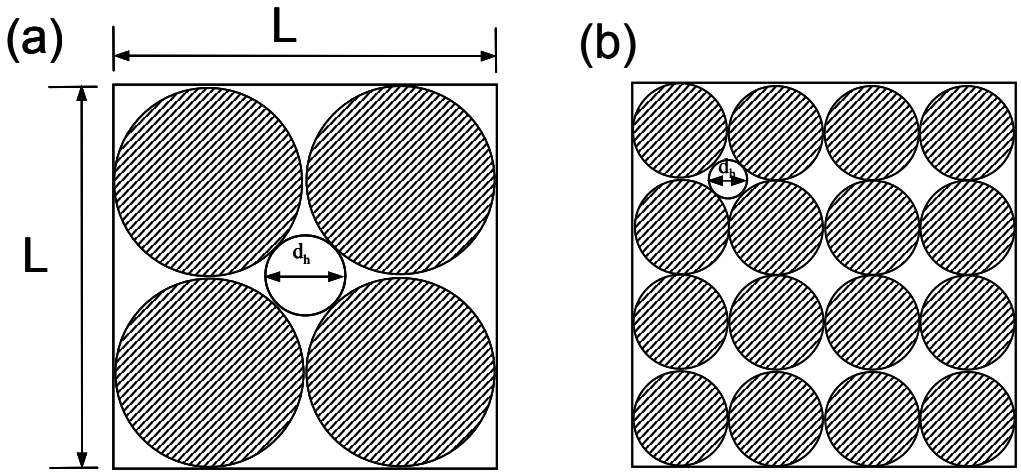

Figure 2-8: Schematic particle beds with the same porosity but different permeabilities, showing two particle sizes in a cross section

The data for the permeability, *K*, indicate a strong dependency on particle size such that the permeability more than doubles for less than a doubling of particle size. The

equal mix sample (comprised of equal masses of two different particle sizes) indicates a strong tendency toward the permeability of the small sized particles. The reason for the variation of permeability can be inferred from Figure 2-8 for two beds with the same porosity. Large particles have a larger permeability than smaller particle sizes because the interface characteristic hydraulic diameter (d_h) for flow between the particles (bed volume/sums of particle surface areas) is greater. It is well known for laminar flow through small diameter pores that the pressure drop for a given flow rate will increase with d_h^{-4}, implying that beds (a) and (b) will have a permeability ratio

$$K_a / K_b = \left[d_{h(a)} / d_{h(b)} \right]^4 = 16 \text{ for } d_{h(a)} = 2 d_{h(b)}$$

The specific surface area, A_S, is a function of the porosity and permeability as given by equation (2-4). For $\varepsilon \approx$ constant, A_S decreases with particle size because A_S is proportional to $K^{-1/2}$. Again referring to Figure 2-8 as an example, the specific surface ratio $A_{S(a)} / A_{S(b)} = 1/4$ for beds with equal porosity but $d_{h(a)} = 2 d_{h(b)}$.

2.4 Calculation of Properties for Mixed Particle Sizes and Comparison with Data

It is known that the particles involved in actual potash products are usually composed of irregularly shaped particles with certain size range. Hence, the property estimations of mixtures of solid particles are necessary. The properties of multi-component particle size mixtures of granular potash can be estimated based on the properties and solid volume fraction of each individual particle size component in the mixture. Two types of mixtures of potash sizes are investigated: one with an equal mass

of a large and small particle sizes and another composed of four component particle sizes with the same distribution of sizes as the original granular potash product.

2.4.1 Calculation of Mixture Porosity

Fundamental and systematic study for the porosity of spherical particle mixtures has attracted the interest of many researches. Yu and Standish (1987) presented a method to calculate porosity of binary mixtures of well-shaken or consolidated beds of particles and they extend this method to calculate porosity of multi-component mixtures of particle sizes when the particle shapes are nearly spherical. Based on this method, the particle diameters, d_{pi} (i.e., for our data i = 1~4) for i component particles can be ordered so that $d_{p1} \geq d_{p2} \geq d_{p3} \geq d_{p4}$ and the fractional solid volume, X_i, will satisfy the equation $X_1 + X_2 + X_3 + X_4 = 1$ where the total volume fraction of solids or packing fraction, p_m, in a bed is $1-\varepsilon_m$ for a well mixed particle bed of porosity ε_m. The relationship between initial packing fraction, p_i, and porosity, ε_i, for each individual particle is defined as

$$\varepsilon_i = 1 - p_i \tag{2-7}$$

Assuming that the dimensionless specific volume (i.e. $(1-\varepsilon_m)^{-1} = p_m^{-1}$) of a multi-component mixture varies linearly with the solid fraction, and there exists only binary interactions among the components. That means the interaction between two sized particles only results in the change of the corresponding fractional solid volume.

The packing fraction of a multi-component mixture of particle sizes is calculated using

$$p_i^T = \frac{p_i}{1 - \sum_{j=1}^{n} (1 - \frac{p_i}{p_{ij}}) \frac{X_j}{X_{ij}}} \qquad (i = 1,2,...,n) \tag{2-8}$$

where p_{ij} and X_{ij} are the maximum packing fraction and the corresponding fractional solid volume when component *i* and *j* make a binary mixture are defined by the equations

$$p_{ij} = \begin{cases} p_i + p_i(1 - p_i)(1 - 2.35 r_{ij} + 1.35 r_{ij}^2) & r_{ij} \le 0.741 \\ p_i & r_{ij} > 0.741 \end{cases} \tag{2-9}$$

$$X_{ij} = \begin{cases} \dfrac{1 - r_{ij}^2}{2 - p_i} & j < i \\ 1 - \dfrac{1 - r_{ij}^2}{2 - p_i} & j \ge i \end{cases} \tag{2-10}$$

where the binary diameter ratios for the various size ranges are defined by the equation

$$r_{ij} = \begin{cases} \dfrac{d_{pi}}{d_{pj}} & i \ge j \\ \dfrac{d_{pj}}{d_{pi}} & i < j \end{cases} \tag{2-11}$$

With this definition r_{ij} is always less than 1 for the size ranges such as those in Table 2-1. The final packing fraction of a mixture, p_m, is the smallest value of p_i^T and the porosity of mixture is defined using p_m.

$$p_m = Min(p_i^T) \tag{2-12}$$

where i = 1,2,3,4 in the case of granular potash particles.

Finally the porosity of the mixture is:

$$\varepsilon_m = 1 - p_m \tag{2-13}$$

This set of equations is used to calculate the porosity of a mixture of spherical particles in a well-mixed bed. The calculated results for ε_m, compared with the measured data in Table 2-3, shows agreement within the uncertainty limits. Because the empirical correlation coming from Yu and Standish (1987) didn't provide uncertainty information, the calculation based on this correlation in the current study does not prescribe an uncertainty.

Table 2-3: Comparison of experimental and calculated values for ε_m

	Shaken		Unshaken	
	Granular product	Equal mix	Granular product	Equal mix
ε_m (Data)	0.395±0.013	0.384± 0.011	0.469±0.008	0.458±0.008
ε_m (Calc.) (Eq.2-12)	0.399	0.382	0.471	0.459

2.4.2 The Calculation of Permeability

An expression for the relation between permeability and porosity is the Carman-Kozeny (CK) equation (Kaviany, 1995). This equation has been used to predict permeability of single particle sizes of nearly spherical shape. In order to apply this equation to the current individual granular potash particle size ranges and mixed particle size ranges, some parameters in the CK equation have to be adjusted to reflect the fact

that the equation was not developed for crystalline particles such as potash. The CK equation for permeability is also used for each particle size,

$$K = \frac{\varepsilon^3}{k_K (1-\varepsilon)^2 A_0^2} \tag{2-14}$$

where, $A_0 = A_{sf} / V_s$. A_{sf} is the solid-fluid interface surface area of the solid particles in a bed with a solid volume V_s.

The Carman-Kozeny coefficient k_k, is defined by

$$k_k = K_0 \tau^2 \tag{2-15}$$

where K_0 is a constant that varies with the particle shape and τ is the tortuosity which is a function of the particle shape and bed porosity. For spherical particles, $A_0 = 6/d_p$, however, potash particles are generally irregular. Thus, a modified or equivalent particle diameter D_p was used to compensate for the non-spherical nature of the potash particles So, Eq. (2-14) can be written as:

$$K = \frac{\varepsilon^3 D_p^{\ 2}}{36 k_K (1-\varepsilon)^2} \tag{2-16}$$

In the current study, a useful value of the equivalent particle diameter could be obtained by multiplying the actual particle diameter by a factor of 1.4. This provided good fit with the experimentally determined permeability. This empirical correction is a shape correction because granular potash particles are cylindrical but not a spherical. For the individual particle sizes, d_{p1}, d_{p2}, d_{p3}, d_{p4}, with mean values d_{p1} = 3.66 mm, d_{p2} = 3.08mm, d_{p3} = 2.58mm, d_{p4} = 2.18mm, and with τ = 1.3 and K_0 = 2.5 for the shaken situation and τ = 1.2 and K_0 = 4.0 for the unshaken situation, the permeability can be

calculated based on modified CK equation (2-16). The permeability calculated via Eq. (2-16) compared well with the experimental data when k_k was set as 4.2 for shaken beds and as 5.8 for unshaken beds.

If the porosity of the mixture and the size distribution are known, the permeability of mixture can be estimated by using a modified CK equation. The equivalent hydraulic diameter concept should be applied in place of the particle diameter d_p. The hydraulic diameter for fluid flow through a porous bed is defined as

$$d_h = \frac{4\varepsilon}{(1-\varepsilon)A_0} \tag{2-17}$$

where $A_0 = A_{sf} / V_s$ is the interface area between the solids (potash particles) and the fluid (air) divided by the volume of the solids.

For a bed of n different particle sizes A_0 becomes

$$A_{0e} = \frac{\sum_{i=1}^{n} \frac{6(1-\varepsilon_m)X_i}{1.4d_{pi}}}{1-\varepsilon_m} = 6\sum_{i=1}^{n} \frac{X_i}{1.4d_{pi}} \tag{2-18}$$

For spherical particles, a bed with a range of particle sizes has an equivalent hydraulic diameter of:

$$d_e = \frac{6}{A_{0e}} \tag{2-19}$$

Finally the permeability of the mixture can be calculated using equation (Kaviany, 1995)

$$K_m = \frac{\varepsilon_m^3 d_e^{\,2}}{36k_K(1-\varepsilon_m)^2} \tag{2-20}$$

With this modified CK model and the statistical distribution of the shaken and unshaken potash mixtures, the calculated permeability of mixture can be determined. Table 2-4 illustrates the results of such a calculation whereby the permeability of two samples (granular product and a equal mix of $2.00<d_p<2.36$ mm and $3.35<d_p<3.96$ mm) are determined experimentally and via Eq. (2-20), with a 16 and 17% discrepancy in each case. In Table 2-4, the uncertainty of calculated results of K_m are not given because the uncertainty of Carman coefficient k_k in the Eq. (2-16) was not provided by Carman.

Table 2-4: Comparison of experimental and calculated values for K_m

	Shaken		Unshaken	
	Granular product	Equal mix	Granular product	Equal mix
$K_m \times 10^8$ (m^2) (data)	2.16±0.09	1.49±0.04	3.47±0.15	2.19±0.06
$K_m \times 10^8$ (m^2) (Calc.) (Eq.2-20)	1.82	1.43	2.89	2.30

2.4.3 Predicting ε_m and K_m for a Equal Mixture of Particles

Assuming that extra fine ($\overline{d}_p = 0.8$ mm) and the largest ($\overline{d}_p = 3.66$ mm) particles are selected to form a binary mixture with 50% solid volume fraction for each particle size range. The methods and correlations presented above can be used to predict the porosity and permeability as shown in Table 2-5.

Table 2-5: Prediction of ε_m, K_m for a mixture

Equal mix $\frac{1}{2}[(\bar{d}_p = 0.8) + (\bar{d}_p = 3.66)]$	Porosity ε_m	Permeability $K_m\,(m^2)$
	0.308	1.363×10^{-9}

The corresponding measurement of ε_m was found to be 0.310 ± 0.006, indicating again that this method of calculating ε_m gives very good agreement with experimental data. Measurement of a corresponding permeability was not performed due to the availability of potash.

2.5 Summary and Conclusions

In this chapter, the important property parameters required to model moisture transfer in granular porous potash by capillarity, gravity and diffusion within a particle bed are investigated experimentally and theoretically for narrow ranges of particle sizes. Porosity and permeability were directly measured with careful attention given to uncertainty. Specific surface area was calculated using the Carman correlation. Experimental results for each narrow range of particle size show the agreement with calculation results (e.g. within ±15% of the test data) for permeability when the Carman-Kozeny equation was used with modifications to account for the crystalline shapes of potash.

For a wide range of particle sizes, such as will be the case for many commercially available products, the potash bed properties are both measured and predicted knowing

the properties of each narrow range of particle size in the mixture. Equations are presented that permit the analyst to predict the porosity, permeability and specific surface area of a mixture of particle sizes given the properties of individual particle sizes. The agreement between the calculated results and measured data is within the experimental test uncertainty for porosity (e.g. less than ±1% of the test data). The porosity in the unshaken or unconsolidated state was found to be somewhat dependent on the experimental procedure in filling the test vessel. For permeability, with a large uncertainty in the modified CK equation, it is within the correlation uncertainty bounds (e.g. less than ±20% of test data).

CHAPTER 3

THE MEASUREMENT OF ONE-DIMENSIONAL MOISTURE CONTENT REDISTRIBUTION WITHIN A POTASH BED

3.1 Introduction

The measurement of moisture content is of great significance for hygroscopic granular materials such as fertilizer products. There are numerous ways to measure moisture content of porous solid particles, and the technique chosen will depend on factors such as the accuracy required and the expense and resources available. Some techniques, such as Near Infrared (NIR) scanning, may allow for in situ moisture measurements in some situations and can give results quickly once they have been calibrated, while others, such as gravimetric techniques, are more time consuming because they require the removal of particle samples from the potash bed to determine the moisture content. On the other hand, gravimetric methods can give very good accuracy and they can be used as a standard, but NIR scanner calibrations are difficult and much less accurate for materials like potash. Furthermore, NIR scanners give only surface moisture signals for a potash bed — they give no information about the average bed moisture content. Methods for determining moisture content in granular materials are compared in Table 3-1.

Table 3-1 Moisture measurement methods for granular material (P.Cancilla, 2001)

Method	Principle	Advantages	Disadvantages
Standard Gravimetric	Drying to evaporate water in material Weighing to get dry sample weight	-High accuracy - Standard Calibration of other methods Low cost	-Time-consuming -bulk volume sample None-automatic measurement
Microwave Phase Shift & Microwave attenuation	Microwave beam changes due to water content	-High accuracy and low detection limit for some materials -Less sensitive to dissolved electrolytes	-High costs -System complexity high -Dependent on bulk density of material
Radio Frequency Transmission	Sensor frequency relates to material dielectric property	-Medium accuracy -Medium investment	-Inter-elemental effects are large -Thickness dependent -Middle costs
Karl-Fisher Titration	Chemical reaction between water and standard reagent	-High accuracy -Wide range substance applications -Moderate cost	-Laboratory scale -Time-consuming -Some materials are limited by chemical reaction
Near infrared (NIR)	Water strongly and selectively absorb infrared radiation	-Medium accuracy for some materials -None-contact with material - Wide application	-High costs -Surface dependent -Beam affected by dust -chemical interference to beam
Nuclear Magnetic Resonance (NMR)	Specific for hydrogen atoms in liquid	-High accuracy over wide moisture range	-Very high cost -Require Nuclear license -Bulk and complex system
Electrical Resistance Tomography (ERT)	Material's electrical conductivity varies with water content	Data Acquisition System available	-Difficult calibration -Special software

This comparison suggests that only the gravimetric and Karl-Fisher titration methods could give the accuracy expected for research work. They both can be independently calibrated. The Karl-Fisher method offers a further advantage that it can be used to determine the moisture content of fertilizer materials that are chemically unstable or volatile such as urea granules and it requires only small samples of less than one gram. The NMR method might be suitable but its very high cost makes it unacceptable. All the other methods must be calibrated against these methods — they can not have an accuracy that is better than these standards.

In this study, the gravimetric method was selected because it is very accurate and it was readily available for experiments.

In order to simulate moisture transfer process in potash bed, it is important to compare simulations with accurately determined initial and final moisture distributions for a large range of test conditions. During this investigation, it was expected that moisture movement will take place in the vertical direction due to diffusion, capillarity and gravity. Due to gravity, moisture content will change more along vertical direction. In order to simplify the experimental and modeling problem, it was assumed that the moisture content redistributed only in the vertical direction; no moisture changes would occur in other directions.

Since there is little or no accurate data available for moisture movement in potash beds all the important bed properties required for an accurate model of moisture

movement must be determined experimentally. These include the bed properties discussed in Chapter 2 as well as the hygroscopic properties of bed saturation, S, versus pore pressure, P_c, and irreducible saturation, S_0. Above the irreducible saturation level ($S>S_0$) moisture will move by capillarity and gravity as well as by molecular diffusion through the interstitial pore air. Below the irreducible saturation level ($S<S_0$) only molecular diffusion through the air is important. Thus any potash bed with one part wet ($S>S_0$) and one part dry ($S<S_0$) will require two different moisture movement models, one for each region. As well, an interface condition will need to be specified if the wet region expands into the dry region or vice versa.

Measurement of accurate moisture contents is the key to determine irreducible saturation and the interface movement condition. Saturation as a function of capillary pressure must be taken from the literature or indirectly deduced from measured data and simulated results because direct measurement of pore pressure in water soluble salts is impractical with standard methods. The development of a new experimental test apparatus and test procedure to determine moisture redistribution is the main task for this chapter.

3.2 Experimental Setup and Test Procedure

3.2.1 Experimental Setup

For this research, we are interested in the spatial redistribution of moisture inside a potash bed due to diffusion, capillarity and gravity. This is a dynamic transport process

with no external moisture interactions; moisture inside the test vessel is conserved at all times because the top, bottom and sides of the whole test vessel are sealed. The test facility for investigation of the one-dimensional redistribution of moisture within potash bed is shown in Figure 3-1.

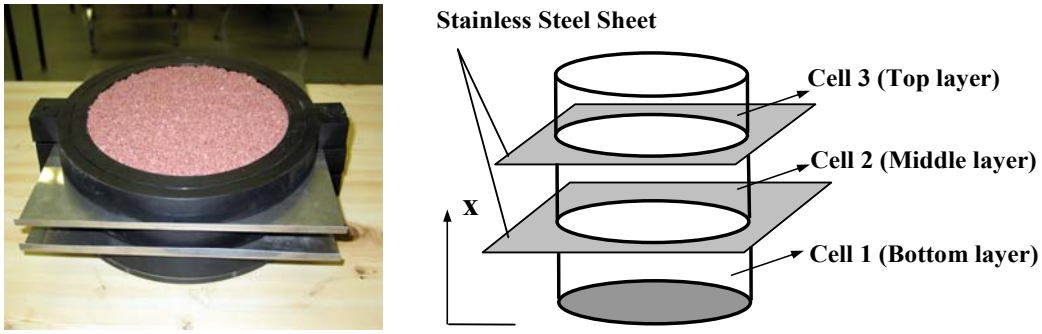

Figure 3-1: Test facility for moisture transfer investigation

This potash bed is comprised of three test cells stacked vertically as shown. The inside diameter of each test cell is 210 mm and the height of each cell is 25 mm. Initially a sample of granular potash with a known moisture content for a specific particle size is placed in each test cell. Very thin stainless steel sheets initially separate each test cell from the adjacent cells. The test is started by removing these two stainless steel sheets without exposing any of the potash inside the test vessel to the ambient air. The test is stopped when these stainless steel sheets are re-inserted between the test cells. The effect of inserting sheets is to separate the different layers of the bed so that the moisture content distribution can be determined. Experiments show that this technique is quite repeatable. To prevent moisture loss or gain during the moisture transfer process and help facilitate the insertion or removal of the stainless steel sheets, O-rings on either side of

each cell are used. The gravimetric method is then used to determine the final moisture content of each test cell.

3.2.2 Experimental Test Procedure

(1) Selection of test samples

Test samples were selected from Lanigan untreated granular potash produced by Potash Corporation of Saskatchewan, Canada. Lanigan untreated granular potash is a granule grade of potash product with size ranges from 2.0mm to 4.0mm diameter. In order to investigate moisture content transport for different particle size distributions, the size particle size ranges shown in Table 2-1 were selected. Each potash sample was initially dried in an oven at 100 °C for about 3 hours to eliminate any moisture due to moisture gain during storage. Then it was covered with a lid to prevent moisture gain while it cooled to indoor temperature. After this process, the potash sample can be considered dry (MC=0%).

(2) Preparation of test sample with pre-certain moisture content

A dry test sample of potash with a small particle size range was taken and weighed to obtain its mass. A known amount of water was added and an electrical stirrer was used to mix the sample and water for 2 minutes so that the particles were of uniform

moisture content. In order to avoid water evaporation, each sample was kept in a sealed container after mixing.

(3) Sample filling procedure

Each empty cell with its corresponding stainless steel sheet was weighed. Then the wet sample was placed into the test cell with a large spoon. Since the moisture content may change a little under the effect of gravity in the mixing container after mixing, gravity induced drainage of water will cause the potash in the bottom of the mixing container to have higher moisture content than that in the top of the mixing container. Samples were therefore taken from all heights in the mixing container. Tight packing of the particles was necessary in the test cell to ensure that the potash bed height would not change in subsequent cell combination and separation processes. Here, the packing effect is equal to the shaken effect in Chapter 2. An auxiliary clamp and lid was used to secure the whole test cell.

(4) Test procedures for moisture transfer within potash bed

This test procedure is illustrated in Figure 3-2. Before each test, each test cell was packed well with a uniformly mixed wet potash sample and was separated from the other two cells by stainless steel sheets. In order to start the test, three test cells were stacked vertically as shown in Figure 3-2, Step 1. Then the stainless steel sheets were slowly pulled out to start the test (Step 2). Duct tape was applied to seal the whole apparatus and

ensure no moisture gain or loss to the surroundings during each test period. After a pre-determined period of time (i.e. several hours), the stainless steel sheets were inserted back between each test cell as shown in Step 3 and the test ended.

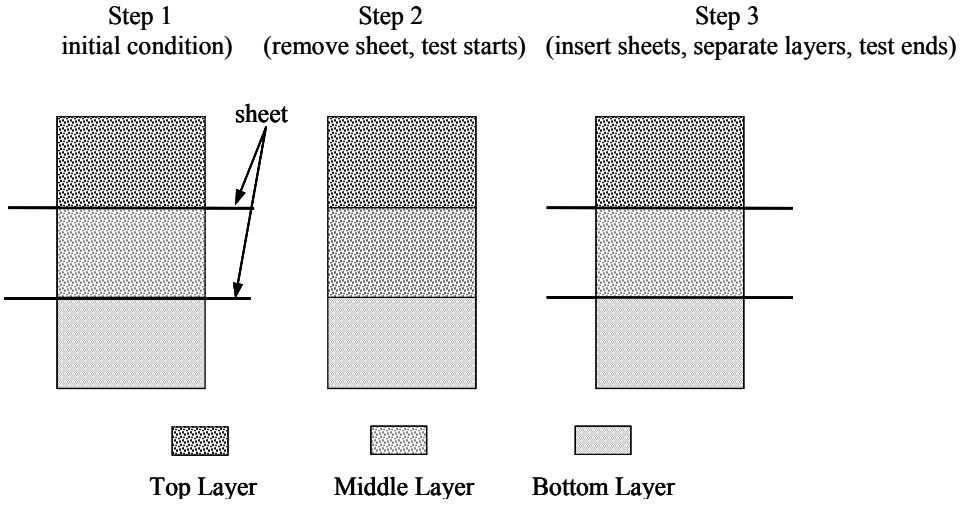

Figure 3-2: Test procedures for moisture transfer within a potash bed

Three additional small aluminium trays were prepared and filled with the same wet potash samples as those in the three test cells at the time the test cells were filled. These three trays with potash samples were weighed and sent to oven for drying. After drying at 100 °C for 15~24 hours (dependent on moisture content investigated) and allowed to cool, each tray with the potash sample was weighed again. From the difference between these two weight measurements and known weight of the empty tray, the initial moisture content for each test cell was calculated.

Each test cell containing a potash sample and its corresponding steel sheet was weighed and sent to the oven for drying at constant temperature. The appropriate drying

time was determined by a series of experiments, which concluded that sample containing less than 6% (w/w) moisture should be dried at 100 °C for 15 hours, and sample with moisture greater than 6% but less than 11% should be dried for 24 hours at 100°C. After drying and cooling, each test cell and corresponding steel sheet was weighted again. Based on these measured data, the final moisture content for each cell after a given moisture transfer time and initial moisture content was determined.

3.3 Uncertainty Analysis of Moisture Content Determination

A systematic uncertainty analysis and evaluation will provide insight into the confidence level for each test result. It can aid in assessing how various possible factors will influence the final moisture content determination.

The following investigations are involved in uncertainty analysis in this chapter: (1) evaluate the reasons for uncertainty generation in each test procedure; (2) estimate the final uncertainty by synthesizing all possible influenced factors in the whole test.

The system is considered one dimensional with three layers from a top cell to a bottom cell. For every layer, if layer is thin, the moisture content can be thought of as having uniform distribution within each layer so that only one described parameter for the moisture content of each layer is needed. This local averaged moisture content denotes the moisture content of all particles within this layer. In the wet sample preparation process, although the weight of water added can be accurately measured with

high precision (±0.001g) and water is uniformly spread into the potash with uniform stirring, it cannot be guaranteed that the water is uniformly distributed. Indeed, the moisture content in the samples on the container bottom part will probably be slightly larger than located at the top of the container, especially when moisture content is high. In addition, moisture may be gained or lost to the air during the sample preparation process. All of these will result in slight discrepancy for the initial moisture content generated under a random taking sample process. However, careful stirring and random sampling technique will minimize the uncertainty for these inevitable factors.

In order to accurately estimate the uncertainty in the initial moisture content due to random sampling, three sets of extra aluminium trays were used and test samples randomly taken from three positions (e.g. surface, middle, and bottom) in container were used to fill each tray. Repeating these experiments and examining the experimental data demonstrated that the maximum discrepancy for the initial moisture content was less than ±0.15%. This value is thought to be the best value of uncertainty for the initial moisture content.

Another possible factor that generates uncertainty is the test starting and ending processes when the stainless steel sheets are removed from and inserted into the test apparatus. During these processes, some very small particles may get removed out of the test cell and this could change the moisture content in a level. Moreover, pulling out and reinserting sheet results in a small amount of particle transfer between adjacent cells and this could also change moisture content. However slowly inserting and removing the

sheets can decrease or nearly eliminate these problems. Tight packing can also decrease the amount of particle transfer. Experimental observations showed that the interchange of particles between cells was limited in a region the size of one particle diameter. For the small particle sizes, particle transfer within adjacent cells appeared to be only in some local positions on the cell surface. Direct measurement of moisture content change due to the reasons above would be very difficult. Although the maximum transferred particle mass was estimated to be about 5% of the original particle mass; the moisture uncertainty due to this type of particle movement is estimated about ±0.1%.

Other factors including sample selection and sample packing variation add another ±0.1%, in terms of uncertainty propagation. Therefore, the total uncertainty in the moisture content measurements at the end of a test is estimated as ±0.2%.

3.4 Summary

In this chapter, an experimental apparatus is developed to evaluate the moisture content and moisture transfer redistribution by diffusion, capillarity and gravity in a small bed of potash fertilizer. The experimental procedures are developed and presented in detail. The gravimetrical method is used to determine moisture content of potash. The uncertainty analysis for the whole test procedure is also evaluated.

CHAPTER 4

THEORETICAL/NUMERICAL MODEL FOR ONE-DIMENSIONAL TRANSIENT MOISTURE TRANSPORT WITHIN POTASH BEDS

4.1 Introduction

Understanding and controlling water migration in hygroscopic porous potash is of importance to insure a high quality potash storage and decreased caking. Peng et al. (1999) found that the critical relative humidity is about 52% for the onset of dissolution of potash, and this is primarily because carnallite ($KMgCl_3 \cdot 6H_2O$) is present in a sufficient concentration (e.g. about 1%) to dominate the low humidity water vapour adsorption and dissolution. As the relative humidity is increased above 52%, increasing amounts of NaCl and KCl dissolution occur, carnallite is first depleted from the surface (e.g. 52% RH for a moisture content of about ω=0.3%). At higher humidities (e.g. 75% RH and about ω=2.5%) halite (NaCl) is depleted. At about 85% RH, the sylvite (KCl) deliquescence point will be reached so the surface humidity can not increase while thermodynamic equilibrium exists. That is, higher ambient air relative humidities will cause all the KCl to be dissolved.

Storage of potash with a time-varying humidity environment will cause water to penetrate into a potash bed. How this water is distributed within a potash bed and causes

dissolution and caking is the basic problem of the potash storage. Questions such as — what is the water penetration depth under a certain storage conditions for a given initial relative humidity and temperature, and what is the risk of extensive caking for a particular range of storage conditions? There is no answer without more research. This chapter will develop a theoretical/numerical model that can be used to predict moisture movement within a potash bed.

In order to develop an accurate model for water accumulation and redistribution within hygroscopic porous potash particles, it is necessary to consider the possible mechanisms that govern water movement and distribution within porous potash. Water transport within porous potash bed can be due to several different mechanisms. These are classified by physical forces and flow regimes.

(1) Water vapour inside the interstitial pore spaces between potash particles will diffuse from regions of higher vapour pressure to lower pressures. Near local equilibrium, dry potash particles will absorb moisture from humid interstitial air with a high vapour pressure. Similarly, moist particles desorb evaporated water vapour to regions of low vapour pressure. Temperature gradients in a potash bed can either enhance or diminish vapour diffusion because the interstitial relative humidity depends on temperature. That means mass transfer is influenced by heat transfer. In actual potash storage, mass transfer is coupled with heat transfer.

(2) When the layers of water molecules on particle surfaces become sufficiently thick to allow liquid movement relative to the solid particles by surface tension gradients and, perhaps, gravity forces, then capillary movement of the surface liquid occurs. Capillary forces on liquid surface films can act in any direction, as determined by the pore pressure gradient, but they may be biased by gravitational forces.

(3) When gravity forces dominate the liquid surface film movement and capillary surface tension effects are negligible, such as occurs in relatively thick, but still finite, film thicknesses, the flow regime is a percolation flow in the direction of gravitational acceleration. Percolation is a random process of water flow downward within thin liquid films interconnected on the particles of a porous media. During this process, some dispersion effects may be evident as the liquid films flow over a random distribution of irregularly shaped particles. That is, percolation flows will on average be in the direction of gravity, but there can be some lateral spreading due to dispersion and local variations in the particle bed permeability.

(4) When the liquid films fill all or most of the pore spaces between particles, any flow is driven by gradients in the static pressure of the liquid minus the gravity pressure. When this flow velocity is small (i.e. the Reynolds number Re_{d_p} is small e.g. less than 10,) then we refer to this as a Darcy type flow because the average superficial velocity will be proportional to this pressure gradient and inversely proportional to the liquid viscosity. Higher Reynolds numbers in the bed flow will lead to more complex flows.

A particular particle bed may be subdivided into spatial regions dominated by one of these flow regimes such that if, for example, in region B shown in Figure 4-1, regime (2) is important then (1) will usually be small or even negligible in region B. Likewise in region B, regime (3) will usually be small or even negligible compared to regime (2). Adjacent to region B may be regions A and C where each of these may be dominated by regimes (1) and (3) respectively. Flow regime (4) is not investigated in this thesis.

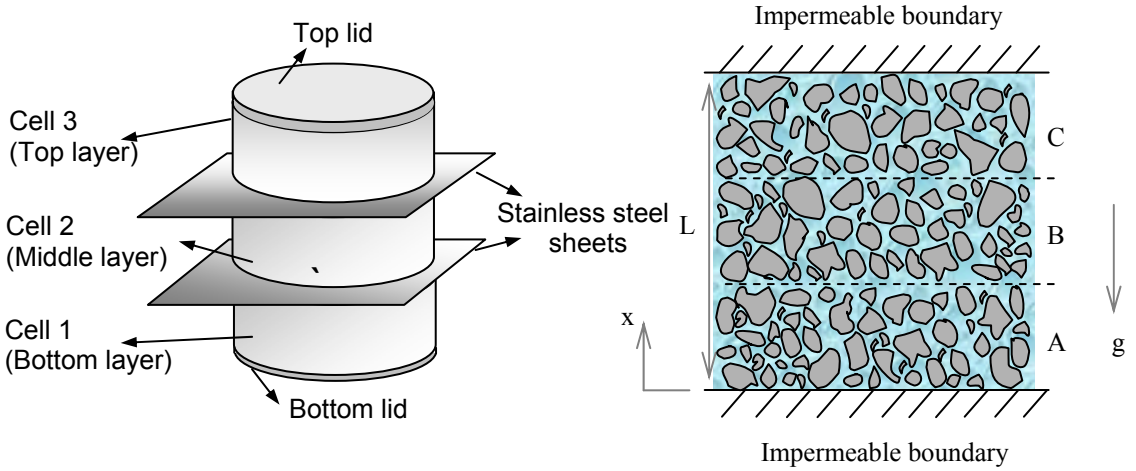

Figure 4-1: Schematic of an isolated particle bed

Each type of flow region in the particle bed, which is dominated by one flow regime, is not, in general, stationary in the bed. The location of a particular flow region is determined by the properties of the bed and its moisture content or liquid concentration. For a potash bed with standard grade particles (average size is 0.8mm), the liquid moisture movement among particles appears to start to be significant at about 10% moisture content. This means that the liquid film will become mobile by capillarity and gravity effects when the moisture content of any point inside a well- packed potash bed is about 10% or higher. For granular potash particles (average size 2.2mm), this threshold

of moisture content for capillarity and gravity effects drops to about 3%. All these critical values (3%, 10%) were obtained after experimental and numerical research.

It is the purpose of this chapter to present the appropriate equations for accurately formulating a physical mathematical model of moisture migration in a potash bed. Then, the numerical solution method of this theoretical model will be used to simulate moisture transport process.

4.2 Problem Statement and Analysis

The necessary condition for the existence of a continuous mobile liquid film is that a relatively large amount of water exists in the pore space. That means the local moisture saturation level, S, is larger than an irreducible saturation, S_0. The moisture saturation, S, is defined as the volume fraction of the porosity occupied by that fluid, i.e.

$$S = \frac{\varepsilon_\beta}{\varepsilon} \tag{4-1}$$

where ε= porosity of the dry granular potash bed=$1-\varepsilon_\sigma$

ε_σ= volume fraction of the dry granular potash bed

ε_β= volume fraction of water in the potash bed

The irreducible saturation, S_0, is the minimum saturation for existence of continuous liquid film movement in potash bed. In the wet region where $S>S_0$, excess water exists as an interconnected mobile liquid film with gravity dominating over capillarity effects. Compared with molecule diffusion of water in air, water motion driven

by gravity effects is about 1000 times larger than diffusion. So, in regions of $S>S_0$, diffusion can be neglected. On the contrary, in the dry region where $S<S_0$, and any liquid is immobile, water vapour diffusion is the only mechanism of moisture transfer. Mass transport is via diffusion only due to the vapour density gradient in the air spaces inside the bed.

When moisture movement occurs across the interface $S=S_0$, it causes the size of the moist and dry regions to change with time. This moisture movement is due to either liquid phase movement or vapour diffusion depending on the moisture content step change across the interface. When the slope of the saturation profile is large at the interface, $S=S_0$, boundary between the wet and dry regions, there will be liquid phase movement. That is, if the slope of saturation profile at $S=S_0, \partial S / \partial x\big|_{S=S_0}$, is higher than an empirical critical value, Sl_0, it is assumed that capillarity and gravity are strong enough to drive the liquid phase across the interface. Under this condition, the interface of the moist and dry regions will move much faster towards the dry part compared to the condition under which moisture transfer across the boundary is by vapour diffusion only. This process will continue till $\partial S / \partial x\big|_{S=S_0} < Sl_0$ and moisture transfer across the boundary is then by vapour diffusion only. The presence of this empirical constant is a necessary condition to determine which water transfer effect occurs at interface and the location of the interface at any time.

In the current study, in terms of saturation, the potash bed can be divided into wet ($S>S_0$) and dry ($S<S_0$) regions. Figure 4-2 shows a schematic of this wet and dry region.

It is assumed that water is present in pores either as continuous liquid film only, or in water vapour form. Correspondingly, different moisture transport equations can be applied to model moisture transfer process in each region and thus to simulate water migration and redistribution.

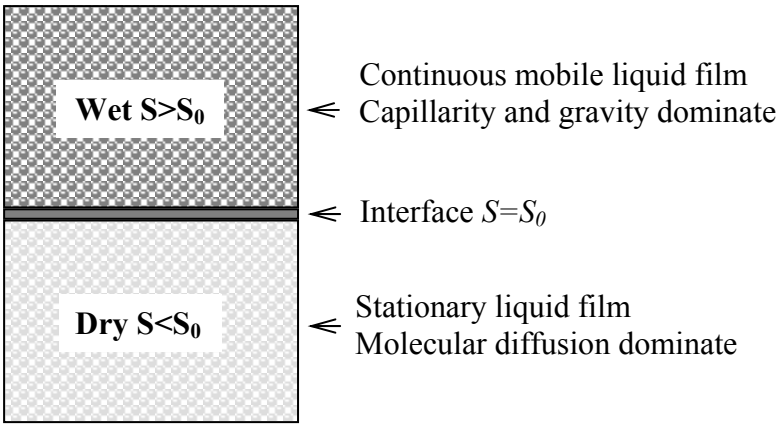

Figure 4-2: Schematic representation of wet and dry regions for moisture transfer within potash beds

4.3 Modeling Assumption and Formulation

The simplifying assumptions used in the mathematical model are:

(1) Moisture transport within the potash bed is one-dimensional in the gravitational direction.

(2) The porous potash, which consists of the solid, liquid and gas phases is assumed to be in local thermodynamic equilibrium (i.e. all phase have the same temperature and pressure at any point within the bed).

(3) The potash bed is rigid and therefore there is no displacement or significant dissolution of particles during the moisture transport process. Therefore, the dry bed porosity is not changed during the moisture transport process.

(4) No chemical reaction occurs during moisture adsorption and transfer processes.

(5) The porous potash bed is homogeneous and isotropic at every point in the bed.

4.3.1 Moisture Transfer by Capillarity and Gravity

When the saturation level in the potash is greater than the irreducible saturation, liquid films will be formed on the surface of the potash particles. Once this occurs, moisture transport can occur via gravity and capillary forces. This continuous film will exist until the local saturation decreases to $S<S_0$. The governing differential equation describing this liquid film movement in a porous bed is:

$$\frac{\partial S}{\partial t} = \frac{1}{\eta_\beta (1-\varepsilon_\sigma)} \frac{\partial}{\partial x}\left[K_\beta \left(-\frac{\partial < P_c >}{\partial S}\frac{\partial S}{\partial x} + \rho_\beta g\right)\right] \tag{4-2}$$

where K_β=permeability of liquid phase in the potash bed (m^2)

η_β=viscosity of water-salt solution in the potash bed, 1.004×10^{-3}(Ns/m^2)

ρ_β=density of water in the potash bed, 998(kg/m^3)

$<P_c>$= volume average pore or capillary pressure (Pa)

The permeability is assumed to follow the empirical equation

$$K_\beta = K_\beta^0 \left(\frac{S - S_0}{1 - S_0}\right)^n \tag{4-3}$$

where S_0 is irreducible saturation, K^0_β is the permeability for saturated flow (S=1) through the granular potash bed. This value is equal to the measurement value of permeability in Chapter 2. n is a positive constant, Whitaker (1980) recommend $2<n<5$. S_0 and n are different for different types of potash and for different packing of particles within a bed. These are determined from the different numerical studies presented in Chapter 5.

Because volume averaged capillary pressure or pore pressure is related to pore space geometry (i.e. pore structure and size distribution), beds of small particles will have a higher capillary pressure than beds of larger particles. This capillary pressure can be expressed by an equivalent static liquid depth as Eq. (4-4).

$$\langle P_c \rangle = \rho_\beta g h \tag{4-4}$$

Experience shows that the parameters that affect capillary pressure on the macro scale are saturation and wetting history of the porous media. The relationship between saturation and capillary pressure can be determined from the height of static liquid under different saturation conditions. In this study, no direct correlation was obtained via experimental measurements, and it is assumed that the capillary pressure relationship is similar to that of a bed of sand because the current particle size range is close the range of sand particles. This relationship, between capillary pressure and saturation for sand, was determined by Ceaglske and Hougen (1937) and modified by Whitaker (1980). This is,

$$\frac{h}{h_0} = 1 - e^{-a(1-S)} + b(1-S) + \frac{c}{(S-S_0)^d} \tag{4-5}$$

where h_0=reference depth =4.9 cm

a=40, b=0.367, c=0.0163, d=1.15.

Substituting Eq. (4-4) and Eq. (4-3) into Eq. (4-2 yields Eq. 4-6:

$$\frac{\partial S}{\partial t} = \frac{\rho_\beta g K_\beta^0}{\eta_\beta (1-\varepsilon_\sigma)} \frac{\partial}{\partial x}\left[\left(\frac{S-S_0}{1-S_0}\right)^n \left(-\frac{\partial h}{\partial S}\frac{\partial S}{\partial x}+1\right)\right] \tag{4-6}$$

The derivative term $\frac{\partial h}{\partial S}$ is obtained from Eq. (4-5). It is more convenient to measure moisture content than saturation. This relationship between moisture content and saturation is given as

$$\omega = \frac{S\varepsilon\rho_\beta}{\rho_s(1-\varepsilon)} \tag{4-7}$$

where ω = moisture content

ρ_s = density of pure potash, 1987 kg/m^3

4.3.2 Moisture Transport via Vapor Diffusion

In the dry region ($S<S_0$), liquid moisture exists in adsorption layer on the particles but this liquid film remains stationary and immobile. Water vapour can only move by molecular or Fickian diffusion in gas-filled pores. This water flux can be modelled by Fick's law of diffusion.

$$J = -D_{eff}\frac{\partial \rho_\upsilon}{\partial x} \tag{4-8}$$

where J = water vapour molecular diffusive flux (kg/m^{2}s)

ρ_v = the density of vapour, kg/m^3

D_{eff} is effective diffusion coefficient. The effective diffusion coefficient can be calculated using the equation

$$D_{eff} = \frac{\varepsilon \cdot D}{\tau} \tag{4-9}$$

where D = the binary diffusion coefficient for water vapour in air, D=0.26x10^{-4}m^2/s

τ = tortuosity =1.1~1.8 for large to small particle sizes (Peng, 1999)

ε = porosity of potash bed

By applying the continuity equation to the water vapour movement, the governing equation which describe the moisture diffusion transport process in the interstitial air space is

$$\frac{\partial(\varepsilon_v \rho_v)}{\partial t} - \dot{m} = \frac{\partial}{\partial x}\left(D_{eff} \frac{\partial \rho_v}{\partial x} \right) \tag{4-10}$$

where ε_γ = the volume fraction of the gas phase

$\dot{m}$ = the moisture phase change rate, kg/(m^{3}s)

The mathematical model must include the liquid phase continuity equation that reflects the process of moisture transfer between water vapour and liquid phase. That is,

$$\frac{\partial \varepsilon_\beta}{\partial t} + \frac{\dot{m}}{\rho_\beta} = 0 \tag{4-11}$$

Mass transport of water vapor results in a change in the local vapor pressure and hence relative humidity. Relative humidity can be calculated by the equation:

$$\phi = \frac{P_v}{P_{v\,sat}} \tag{4-12}$$

where ϕ = relative humidity of air

P_v = vapour pressure (Pa)

$P_{v\,sat}$ = saturation vapour pressure (Pa)

Under the experimental conditions where the pressure is not so high, water vapour behaves as an ideal gas and the following equation of state can be used to calculate the vapour pressure in terms of ideal gas law as follows:

$$P_v = \rho_v R_v T \tag{4-13}$$

where R_v = gas constant =462 J/(Kg·K)

T = temperature of potash bed (K)

The saturation water vapour pressure is calculated by using the empirical equation shown in the ASHARE Handbook Fundamentals (1997). The saturation pressure, P_{vsat} over liquid water for the temperature range from 0 to 200 °C and over ice for the temperature range of -100 to 0 °C are respectively given by

$$ln(P_{v\,sat}) = \frac{C_1}{T} + C_2 + C_3 T + C_4 T^2 + C_5 T^3 + C_6 T^4 + C_7 \ln T \tag{4-14}$$

$$ln(P_{v\,sat}) = \frac{C_8}{T} + C_9 + C_{10} T + C_{11} T^2 + C_{12} T^3 + C_{13} \ln T \tag{4-15}$$

where T = absolute temperature, K= °C +273.15 and the empilrical constants

C_1= -5.674359×10^3, C_2= 6.3925247, C_3= -9.677843×10^3, C_4= 6.2215701×10^{-7}

C_5= 2.0747825×10^{-9}, C_6= -9.4840240×10^{-13}, C_7= 4.1635019, C_8= -5.8002206×10^3,

C_9= 1.3914993, C_{10}= -4.8640239×10^{-2}, C_{11}= 4.1764768×10^{-5},

C_{12}= -1.4452093×10^{-8}, C_{13}= 6.5459673

Give the most accurate predictions available

4.3.3 Adsorption/Desorption Modeling

The research work of Peng et al. (1999) studied the interaction between potash and moisture at equilibrium both experimentally and theoretically. Peng's research showed that there is a critical relative humidity around 52% at which point condensation begins to occur. When totally dry potash is exposed to air with a relative humidity lower than this critical humidity, potash can adsorb some moisture, but water vapour condensation will not occur. However, when the relative humidity is higher than the critical value, the chemical potential difference between the water vapour in the air and the water in the surface aqueous solution will provide a diffusion driving force, and the water vapour will condense continuously on the surface until a chemical equilibrium is reached. If potash is exposed to a relative humidity higher than 85% or the deliquescent point for KCl, the water vapour condensation will continue until all the potash dissolves.

Zhou (2000) summarised Peng's work and gave some simplified equations to describe the adsorption/desorption isotherm of granular potash. Zhou's expressions adequately represent the situation where there are slight variations in the chemical composition of the surface layer of potash on various adjacent particles. Figure 4-3 shows

a typical plot of moisture content of potash versus relative humidity at one temperature based on these equations.

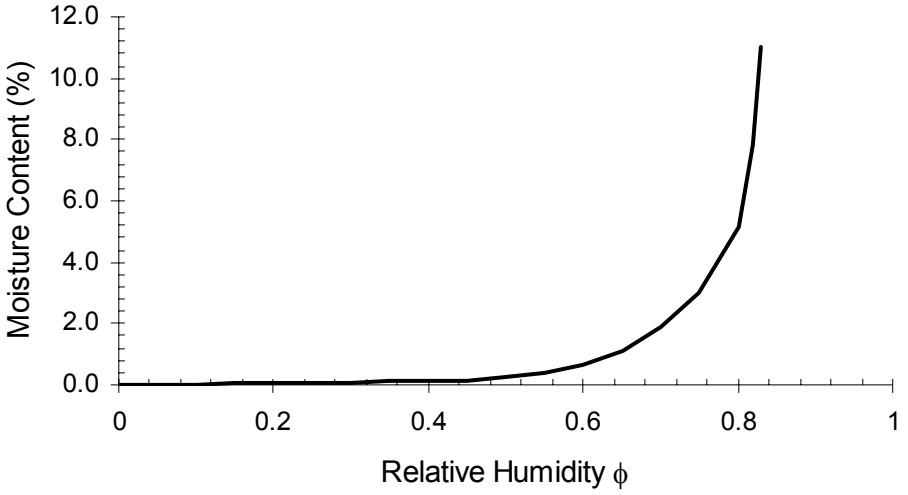

Figure 4-3: Typical isotherm of moisture content for potash (T=20°C) as a function of relative humidity

For the adsorption of water, the best fit analytical expressions for moisture content of potash at equilibrium conditions (Zhou, 2000) is

$$\frac{\omega_e}{\omega_m} = \frac{C \cdot \phi}{(1-\phi)[1+(C-1)\phi]} \qquad (\phi < 45\%) \qquad (4\text{-}16)$$

where ω_e = the equilibrium moisture content

ϕ = the relative humidity

ω_m = 0.2% (the empirical constant)

C =1.54 (the empirical constant)

For the liquid film of water, the desorption equilibrium moisture content isotherm is expressed using the polynomial empirical fit equation (Zhou, 2000). This is:

$$\omega_e = \frac{1}{d'+e'\phi + f'\phi^2 + g'\phi^3} \qquad (45\% \le \phi < 85\%) \qquad (4\text{-}17)$$

d', e', f' and g' are constants that depend on the temperature of the surface layer of the potash and these are determined by curve fitting using Peng's theoretical model for potash at equilibrium. In his study, they were determined as d'=7609.3, e'=-28842.6, f'= 36902.2 and g'=-15885.3 at 20 °C.

In order to characterise the mass of water in potash particle beds that has been deposited by adsorption and condensation, the relationship between moisture content and water mass that change phase per unit volume is given by

$$\omega = \frac{\Delta m_\omega}{m_{dry}} \qquad (4\text{-}18)$$

where Δm_ω = the mass of water per unit volume (kg/m^3)

m_{dry} = the mass of dry potash per unit volume (kg/m^3) = 1200

The rate of moisture accumulation or rate of phase change, $\dot{m}$, in the moisture transport process of potash bed is calculated using the equation

$$\frac{\dot{m}}{m_{dry}} = -\frac{d\left(\frac{\Delta m}{m_{dry}}\right)}{dt} = -\frac{d(\omega)}{dt} = -\frac{d(\omega)}{d\phi}\frac{d\phi}{dt} \qquad (4\text{-}19)$$

4.3.4 Moisture Transfer at the Interface ($S=S_0$)

In the interface region between wet and dry areas of the bed, liquid phase movement and vapour diffusion are coupled. The resulting moisture transfer process is complex. The spatial grid point adjoining wet and dry regions will distinguish which one adopts the capillary model and which one uses the diffusion model.

In order to describe how the boundary is numerically established, a control volume method is used to discretize the governing set of partial differential equations. Figure 4-4 illustrates the control volume configuration at the interface.

As shown in Figure 4-4, control volume, “a” and “a'” indicate two adjacent regions that are located just on each side of interface. The regions where the liquid phase movement equation and the vapour diffusion equation are applied are determined based on the value of $\partial S / \partial x \big|_{S=S_0}$ and are shown in Figure 4-4 for both $\partial S / \partial x \big|_{S=S_0} < Sl_0$ and $\partial S / \partial x \big|_{S=S_0} \geq Sl_0$. Sl_0 is an empirical constant (m^{-1}) introduced to determine the rate of the interface mass flux between the wet and dry regions defined by $S=S_0$. This moving boundary problem requires a curtain build up of moisture at the boundary before it moves. Numerically this movement is in space descrete steps. The value of Sl_0 depends on the grid size and it is found by comparing measured data with simulation runs in a parameter sensitivity study.

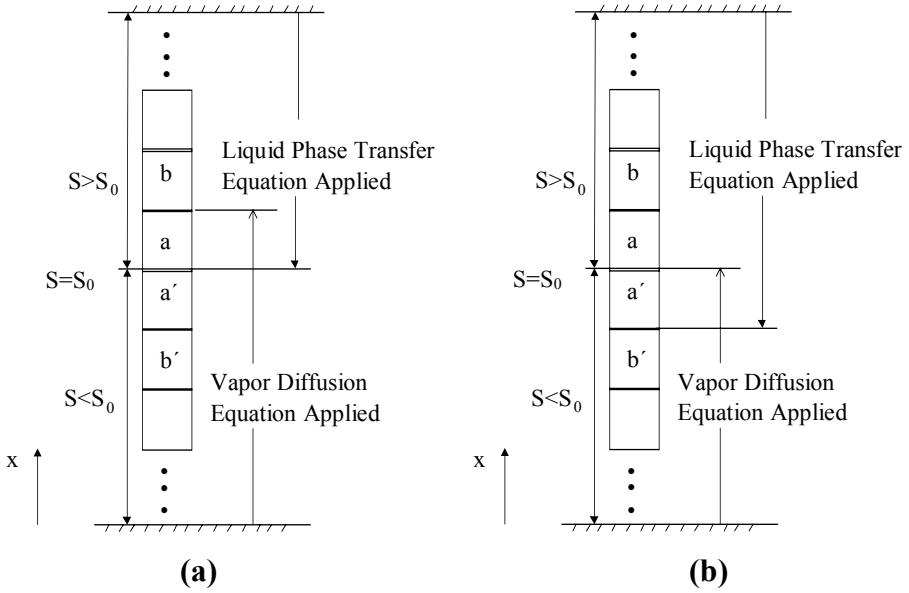

Figure 4-4: Schematic of moisture transfer near the interface S_0 using descrete nodes

(a) $\left.\frac{\partial S}{\partial x}\right|_{S=S_0} < Sl_0$, **(b)** $\left.\frac{\partial S}{\partial x}\right|_{S=S_0} \geq Sl_0$

When $\partial S / \partial x\big|_{S=S_0} < Sl_0$, the moisture transfer across the interface is only by vapour diffusion. The region "a" is the point where vapour diffusion and liquid phase movement are coupled. The liquid phase transfer equation applied in region "a" should be modified by addition of a source term that takes into account the evaporation of the liquid phase.

$$\frac{\partial S}{\partial t} = \frac{\rho_\beta g K_\beta^0}{\eta_\beta (1-\varepsilon_\sigma)} \frac{\partial}{\partial x}[(\frac{S-S_0}{1-S_0})^n (-\frac{\partial h}{\partial S}\frac{\partial S}{\partial x}+1)] - \frac{\dot{m}_b}{\varepsilon \rho_\beta} \tag{4-20}$$

where $\dot{m}_b$ is the rate of phase change indicating the amount of liquid phase that evaporates at boundary interface. The corresponding vapour diffusion equation applied in region "a" is,

$$\frac{\partial(\varepsilon_\gamma \rho_v)}{\partial t} = \frac{\partial}{\partial x}\left(D_{eff} \frac{\partial \rho_v}{\partial x} \right) + \dot{m}_b \tag{4-21}$$

When $\partial S / \partial x\big|_{S=S_0} \geq Sl_0$ the moisture transfer across the interface $S=S_0$ is by means of liquid phase movement. The region “a"’ is the point where vapour diffusion and liquid phase movement are coupled. Equation (4-20) is then applied to region “a"’.

4.4 Initial and Boundary Conditions

The appropriate initial and boundary conditions for a one-dimensional porous potash bed with the presence of a continuous moisture migration in the internal bed, but no infiltration or penetration through the top and bottom boundaries have to be considered in these simulations. The selection of the mathematical formulation is strongly dictated by a physically realistic representation of the studied region. The most important initial condition is the initial moisture content profile $\omega_0 (x)$ along the height of potash bed. The saturation can be calculated from Eq. (4-7) with known moisture content distribution, and the initial value of volume fraction of water also can be calculated from equation

$$\varepsilon_\beta = \frac{\omega \rho_s (1-\varepsilon)}{\rho_\beta} \tag{4-22}$$

Under the assumption of constant temperature, one moisture content of potash will correspond to only one relative humidity as given in equation (4-16) and (4-17). The vapour density is correspondingly calculated from a known relative humidity and temperature.

When the wet and dry regions are specified, boundary conditions can be set. In the region $S>S_0$ in Figure 4-2, the liquid phase transfer Eq. (4-6) applies and the boundary conditions at top and bottom boundaries of the region are set so that

$$-\frac{\partial h}{\partial S}\frac{\partial S}{\partial x}+1=0 \tag{4-23}$$

which implies that the gravity and capillarity forces are balanced at the boundary. For the vapour diffusion region, $S<S_0$, the boundary condition should satisfy the condition that the mass flux of vapour diffusion is set to zero at the top and bottom boundaries. This can be prescribed by

$$\frac{\partial \rho_v}{\partial x}=0 \tag{4-24}$$

The numerical algorithm and property values used in the simulations are presented in Appendices C and D.

4.5. Summary

In this chapter, a model based on Whitaker's theory (1977) is introduced to simulate one-dimensional transient moisture transport in homogeneous porous potash beds. Unlike other water transport models reported in literature, this model fully accounts

for diffusion, capillarity and gravity effects within different spatial transport regions which are represented by two kinds of different moisture transport mechanisms. The irreducible saturation is used to define the regions for these two models. This model is particularly useful for improving our understanding of the actual moisture migration process in potash.

The applicability of this model is limited to isothermal conditions. The methodology of this work can provide a starting point for multidimensional moisture transport in heterogeneous potash beds with heat transfer.

CHAPTER 5

COMPARISONS BETWEEN NUMERICAL SIMULATIONS AND DATA

5.1 Introduction

To calculate the dynamic transfer process of water within potash bed by diffusion, capillarity and gravity effects, the water transfer region is decomposed into wet and dry regions. For different regions, a different water transfer mechanism is used. It is assumed that irreducible saturation, S_0, separates the wet and dry regions. Therefore, one of the most important steps is to determine irreducible saturation.

The objective of this chapter is to present the validation of the numerical model of moisture transport for the prediction of water transfer within potash bed by accounting for diffusion, gravity and capillarity effects by comparing simulation results with accurate measurements. Firstly, it is shown how irreducible saturation versus particle size is determined using both experimental measurements and numerical calculations in a sensitivity study. Then, a correlation is developed for a mixture of particle sizes in granular potash knowing the irreducible saturation of each individual particle size range and the corresponding fraction in the mixture. As well, some illustrative simulation

results are presented to show transient moisture transfer. Finally, comparison between experimental data and numerical computation shows the accuracy of model.

5.2 Determination of Irreducible Saturation

5.2.1 Irreducible Saturation versus Particle Size

Direct steady state measurement of pore pressure and irreducible saturation is problematic in a salt bed such as potash because potash will undergo some degree of dissolution for local relative humidities greater than 52% and moisture contents greater than 0.1% by mass. To overcome this problem an indirect transient test method was used to determine S_0. In this research, S_0 was determined by performing many experiments with potash beds at various moisture contents with each initial condition close to the irreducible saturation. The transient moisture distribution data obtained were compared to the results of corresponding numerical experiments for saturation, S. The corresponding moisture content, ω, at any saturation S, (including ω_0 for $S = S_0$) is calculated using the equation (4-7).

The granular grade of potash with a total particle size range 2.0 to 3.96mm was subdivided into four size ranges 2.00 mm<d_p<2.36 mm, 2.36 mm<d_p<2.80 mm, 2.80 mm<d_p<3.35 mm and 3.35 mm<d_p<3.96 mm. In addition, an extra fine particle size with average diameter 0.8mm was also used in this research to investigate initial saturation. For each particle size range visual observations revealed the onset of the drainage water

at different moisture contents. For small particle sizes (e.g. diameter 0.8 mm), this liquid moisture movement only started to be significant at about 10 % moisture content. That is, for any point inside a bed at about 10 % moisture or higher in a well packed potash bed, capillarity and gravity will cause gravitational movement of the liquid. For the granular particle with average size 2.2 mm in a well packed bed, this moisture content threshold for capillary and gravity effects drops to about 3%. The range of moisture contents corresponding to testing four particle size ranges (2.0mm~3.96mm) and the extra 0.8mm that were used to determine ω_0 was 2 %~10 %.

The mathematical/numerical model (Chapter 4) was used to determine the irreducible saturation for each particle size by comparing simulations with measured data for moisture content. The numerical calculation procedure is as follows.

1) Input the initial and final moisture content profile using measured moisture content and time. Calculate initial and final saturation distribution and the corresponding value of volume fraction of water.

2) Assume a value of S_0, then knowing the initial saturation distribution predict the size of the wet and dry regions.

3) For the wet region, the capillarity and gravity model is applied. For the dry region, the diffusion model is applied. At the interface, capillarity and gravity model is coupled with the diffusion model.

4) Obtain the final value of moisture content at specified test duration time. Adjust S_0 and repeat the procedure above until the final predicted moisture content for each layer agrees

with the experimental data. When the difference between the simulated moisture contents and all the experimental data is minimum, then the best value of S_0 will be known for a given particle size.

In order to investigate the sensitivity of the exponent n in equation (4-3) that relates saturation to pore pressure, another parameter sensitivity analysis was conducted. Whitaker (1980) suggested that n should have the range $2 \leq n \leq 5$. Comparing results with changes in n, causes the irreducible saturation to change slightly. Utilizing the least-square method to select the best fit values of S_0 and n in a parameter sensitivity study, the optimum empirical constants were selected for the analytical/numerical model. Comparison of numerical results with experimental data is limited within ±0.2% uncertainty. These research results showed that the best fit n was 3 for large particle sizes (2.0 mm< d_p <3.96 mm), 4 for small particle sizes d_p<1.00 mm. The best fit irreducible saturation, S_0, is presented in Figure 5-1. A correlation between irreducible saturation and particle size is developed by using curve fitting software (TableCurve). TableCurve's non-linear least-squares Gaussian fitting was used to establish this best fit curve. This correlation is

$$S_0 = 0.047 + 0.162 / d_p^2 \qquad (5\text{-}1)$$

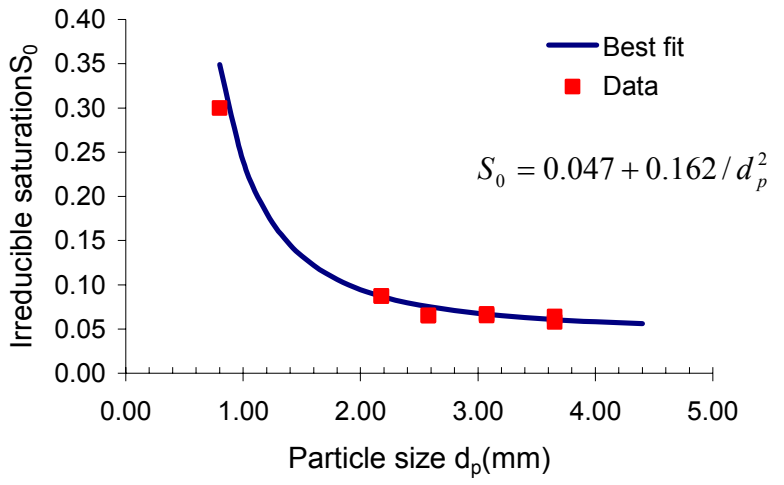

Figure 5-1: Irreducible saturation versus particle size

5.2.2 Irreducible Saturation for Mixtures of Different Particle Sizes

In this section, an empirical correlation between individual particles and mixtures of granular potash is developed for the prediction of irreducible saturation of the granular potash product, which contains a wide range of particle sizes. It is hypothesized that a good correlation can be expressed as

$$S_{0m} = \int_0^\infty S_0(d_p) \cdot f_x(d_p)\, d(d_p) \qquad (5\text{-}2)$$

where, $S_0(d_p)$ is a function of particle size d_p, shown in Figure 5-1, and $f_x(d_p)$ is a mass or volumetric distribution function. That is, f_x is the particle size derivative of cumulative mass fraction distribution function, shown in Figure 2-6. The slope of the best fit cumulative mass fraction distribution curve with respect to particle size gives the mass or volumetric distribution function, f_x. This distribution, $f_x(d_p)$, is shown in Figure 5-2. Due to the large uncertainty in the moisture transfer experiments used to determine S_0 for

unshaken particle sizes, no correlation is presented in this thesis for the unshaken mixtures of particle sizes.

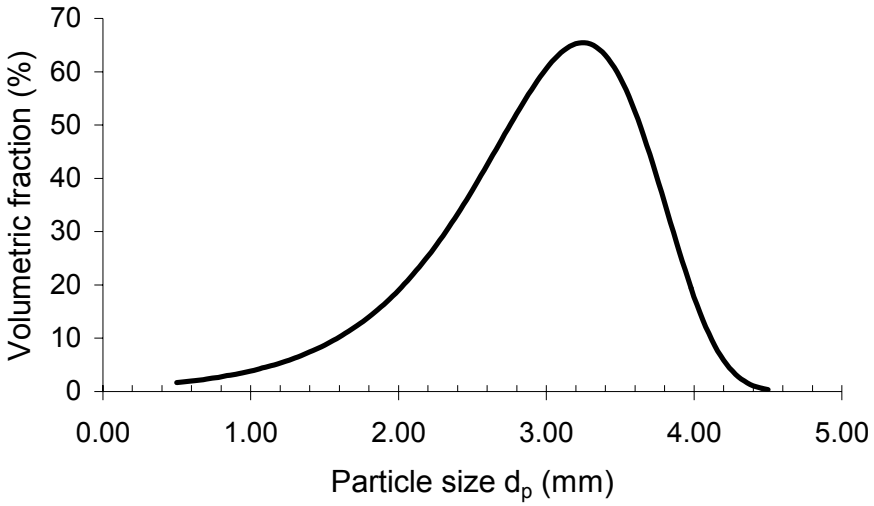

Figure 5-2: Volumetric distribution versus particle size for the original granular product

In the experiment the extra fine ($\overline{d}_p = 0.8\,\text{mm}$) and largest ($\overline{d}_p = 3.66\,\text{mm}$) particles were selected to form a binary mixture with 50 % solid volume fraction for each particle size using equation (5-2), the irreducible saturation is be predicted for this binary mixture as shown in Table 5-1. The experimental S_{0m} is a value determined using experimental data and a parameter sensitivity study in the numerical simulation as described previously in section 4.3.4 for S_0. Table 5-1 compares these two independent methods of obtaining S_{0m}.

Table 5-1: Irreducible saturation S_{0m} for a binary mixture of particle sizes

Equal mix $\frac{1}{2}[(\bar{d}_p = 0.8) + (\bar{d}_p = 3.66)]$	Predicted S_{0m}	Experimental S_{0m}
	0.179	0.182

5.3 Moisture Distribution Numerical Prediction and Experimental Comparison for One-Dimensional Transfer

The numerical model was validated by comparing the simulation results with experimental data through some case studies. If the simulation provides a reasonably accurate calculation of the moisture content compared to the experimentally measured values, the mathematical model is validated. In this study, the four size ranges of potash particle in section 5.2.1 were investigated. Several comparisons are presented here. These graphs show moisture content changes with time. The line ω_1, ω_2 and ω_3 respectively denote the simulation results for top layer, middle layer and bottom layer. Marks denote experimental data.

The first test condition was for a three layer potash bed where each layer has different moisture content. Figure 5-3 shows the typical transient moisture profile for a potash sample with a particle size distribution of 2.00 mm to 2.36 mm. The measured initial moisture content for the three layers, from top to bottom are 4.53 %, 3.73 % and 2.94 % respectively. After 60 minutes the moisture content has redistributed to 3.71 %, 3.84 % and 3.65 % from top to bottom. When the moisture content transfer was

continued for another 60 minutes, the moisture content had further redistributed to a final distribution of 3.57 %, 3.70 % and 3.94 % from top to bottom.

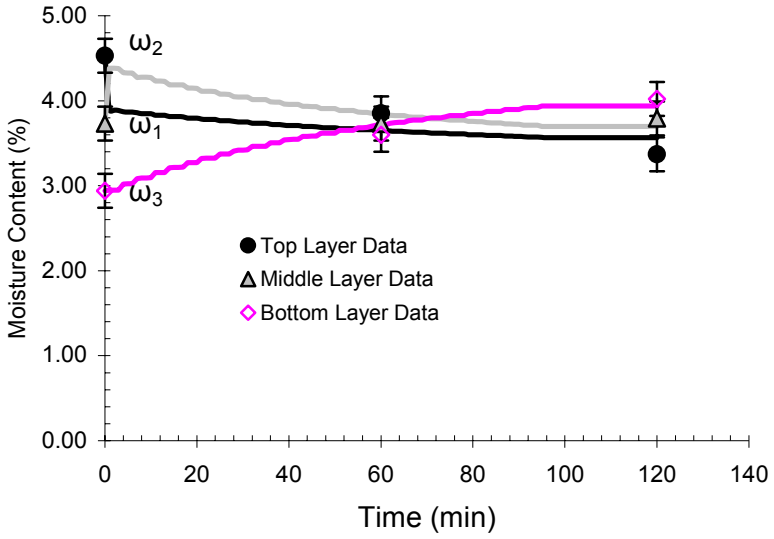

Figure 5-3: Comparisons of transient moisture content profile between simulation and experimental data (t=0, 60, 120 min.) for granular potash with d_p=2.00~2.36mm

For this type of potash, the empirical parameters used in the numerical model (Chapter 4) were τ=1.1, n=3, S_0=0.087 and Sl_0=135/m. All selected parameters used in the numerical model were determined by performing many numerical simulations and comparing these simulation results with experimental data using parameter sensitivity studies. The final simulation results fitted well with all the experimental data for 40 sets of data. Only this set of parameter presented can result in a good fit for all the experimental data. The sensitivity studies show that, for the potash particle sizes ranging from 2.00 to 3.96 mm, S_0 is the most important parameter used in the numerical model while Sl_0 is important only when there is an initial large step change of moisture content between each layer (with one layer being very wet, the other layer being at a saturation

level less than S_0). The 95 % test data confidence limits show good agreement between all the test data and simulation results as illustrated in Figure 5-3. Comparisons between the predicted moisture contents with six sets of experimental data in this case study indicate each has good agreement within a ±0.2 % uncertainty bound. Figure 5-3 may also imply that it would be desirable to obtain more experimental data, especially for short time periods, i.e. 5 to 15 minutes after the start. This problem of getting data at any time has been better addressed with a new moisture sampling method introduced after this thesis work was completed. It also showed good fits for various times.

The second test case was for a potash bed in which the bottom two layers are almost totally dry (i.e. the initial moisture content of bottom two layers has a typical dry value about 0.02 %). The top layer was at a much higher moisture content compared with bottom two layers. Two different top layer moisture contents were selected to compare with the numerical model: one moisture content was relatively low at about 3 % and, the other was about 5 %.

Figure 5-4 and Figure 5-5 respectively show the transient moisture content distribution profile for a granular potash bed with average particle size of 2.2 mm at moisture content of 2.85 % and 5.33 % respectively. For an initial top layer moisture content of 2.85 % which corresponds to S_0 of 0.087, for an average particle size of 2.2 mm, the moisture migration within potash bed is only by vapour diffusion. Here the simulation results, shown in Figure 5-4, agree with experimental data within the bounds of experimental uncertainty. Under the test condition with the top layer initial moisture

content larger than 5 %, liquid film is able to move within the potash bed due to capillary and gravity force effects as well as by vapour transport in the interstitial air.

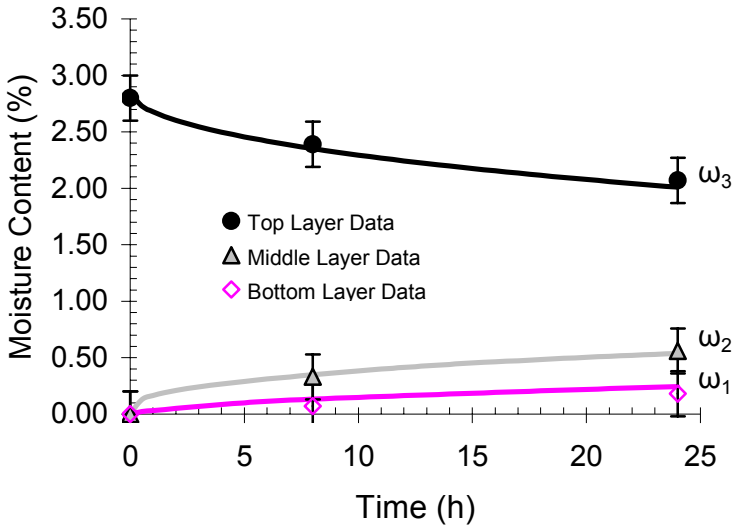

Figure 5-4: Comparisons of transient moisture content profile between simulation and experimental data for granular potash (average d_p=2.2mm and initial MC=2.85%)

The comparison in Figure 5-5 implies somewhat different moisture transfer phenomenon. That is, the one dimensional vapour diffusion or capillary and gravity effects, as modeled in Chapter 4, no longer gives accurate predictions of moisture content. The simulated results under-estimate the moisture content of bottom layer, over-estimate the moisture content of the middle layer, and correctly predict the moisture content of top layer. After drying the whole bottom cell, some localised caking was found to indicate local areas with much more caking than others at the same height in the bed. The discrepancy between the simulation and the data in Figure 5-5 is caused preferred drain down columns inside the particle bed. It is interesting to find that the average value

of simulation result for middle and bottom layer agree well with data. More experimental and analytical study should be done to further investigate this three dimensional drain down effect.

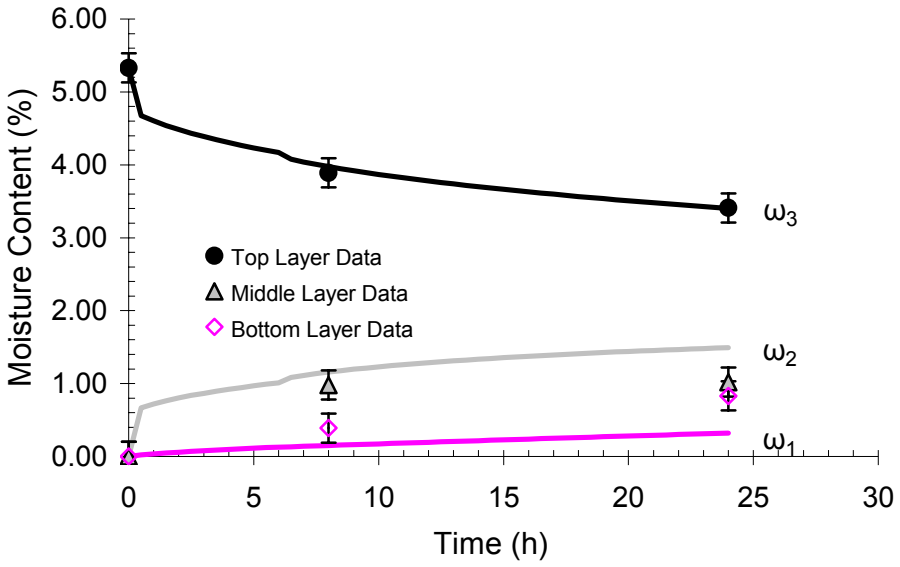

Figure 5-5: Comparisons of transient moisture content profile between simulation and experimental data for granular potash (average d_p=2.2mm and initial MC=5.33%)

In order to further compare numerical model for predicted moisture transfer and measured data, a potash bed with smaller particle size (d_p =0.8 mm) was investigated. Similar to the above case study, the bottom two layer moisture contents were dry with less than 0.02 % moisture content. The top layer potash had an initial moisture content of 5.89 % and 11.0% and the results of these tests are shown in Figure 5-6 and 5-7. For this type of potash, the empirical parameters used in the numerical model were τ=1.8, n=4, S_0=0.30 and Sl_0=175/m. Because diffusion processes are a very slow, there would be no

obvious change in the bed moisture content within short time duration. Hence, these tests are performed for a 24 hour period.

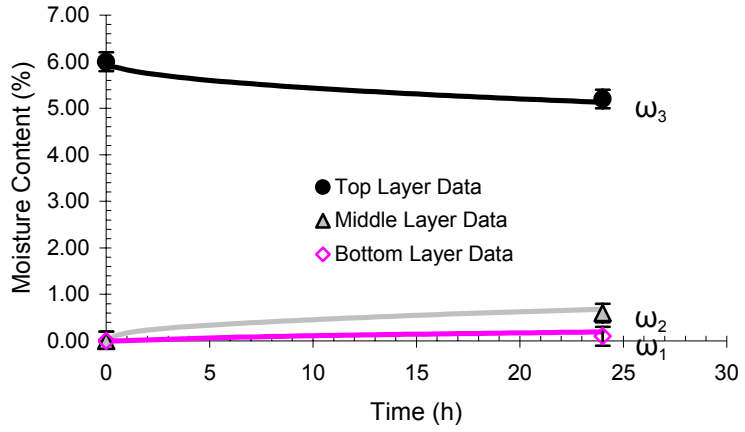

Figure 5-6: Comparisons of transient moisture content profile between simulation and experimental data for standard potash (average d_p=0.8mm and initial MC=5.89%)

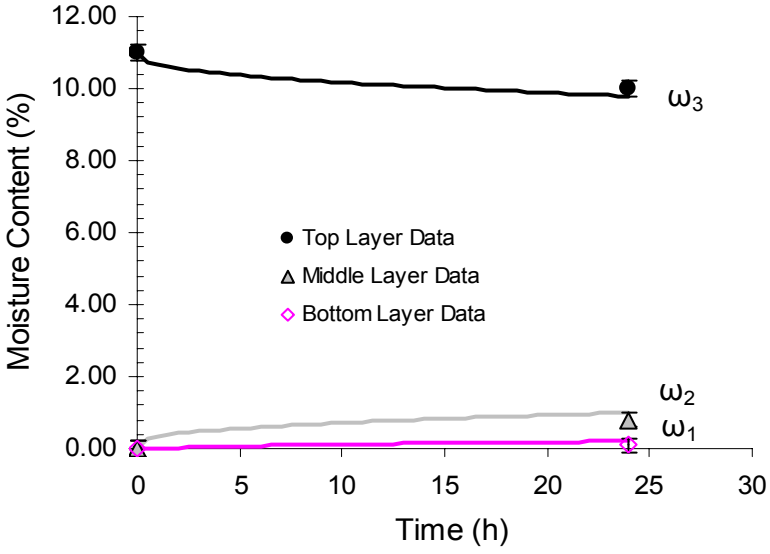

Figure 5-7: Comparisons of transient moisture content profile between simulation and experimental data for standard potash (average d_p=0.8mm and initial MC=11.0%)

Both numerical simulation and experimental observation indicate that the depth of moisture penetration by liquid film movement from top layer to middle layer is only 1-2 mm. This is can be observed from local caking regions after drying the test cells. Caking occurs where moisture has penetrated. It was found that much less moisture was transferred for the smaller particles compared with large of particles under similar conditions.

To show the difference of spatial moisture content during moisture transfer process for different particle sizes, moisture transfer was simulated for two different particle sizes with uniform initial moisture contents 4 %, 3 % and 2 % on the cells from top to bottom. Figure 5-8 shows a comparison of the simulated spatial moisture content profiles at different times for two particle sizes with average diameters 2.18mm and 3.70mm. It can be seen from this graph that moisture transfer for the smaller particle size particle is much slower than that of the larger particle size.

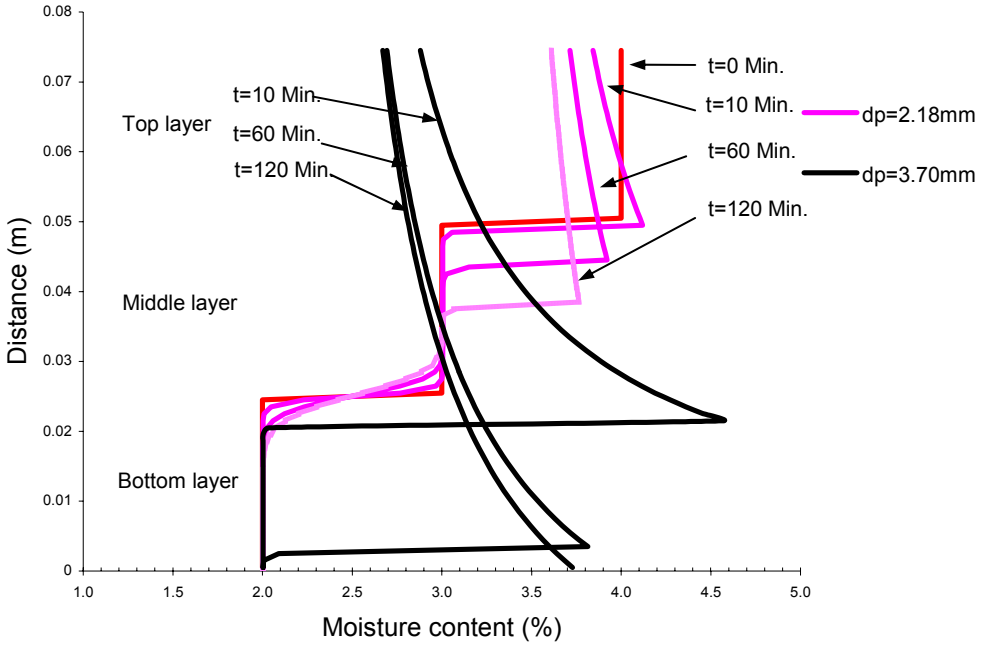

Figure 5-8: Simulated spatial moisture content distribution for different particle size with d_p=2.18mm and d_p=3.70mm

5.4 Bond Number

Capillary, gravity and viscous forces interact to define the pattern and region of moisture transport, as well as the final moisture content distribution. An accurate evaluation of these terms may lead us to obtain physical representation of the relationship between irreducible saturation and particle size distribution. In order to understand the influence of different forces during the moisture transfer processes, the ratios between different forces can be expressed as dimensionless groups. In the current research, the Bond number is used to reflect the relationship between capillary force and gravity force.

The Bond number (N_{Bo}), which relates to the relative strength of gravitational and capillary forces, is defined as

$$N_{Bo} = \frac{\rho_g \left(\frac{\rho_l}{\rho_g} - 1 \right) g\, d^2}{\sigma} \tag{5-3}$$

where ρ_l = liquid density (kg/m^3) = 998 kg/m^3

ρ_g = gas density (kg/m^3) = 1.2 kg/m^3

σ = surface tension (N/m) = 0.072 N/m

g = gravitational acceleration constant (m/s^2) = 9.8 m/s^2

d = characteristic diameter of flow channel (m)

For vertical moisture transport within porous potash bed, the Bond number (N_{Bo}) takes into account the balance between gravity and capillary forces and it is directly proportional to the square of characteristic diameter of the flow channel. Here, particle size is used to describe this characteristic diameter of flow channel. Thus, the Bond number (N_{Bo}) can also be a spatially variant parameter depending on particle size distribution.

Due to the relationship between Bond number and particle size, in order to find the possible relationship between Bond number and irreducible saturation, it is considered that a relationship between irreducible saturation and Bond number is similar to the relationship between irreducible saturation and particle size. This relationship is of the form

$$S_0 = A + B / N_{Bo} \tag{5-4}$$

where A and B are two unknown coefficients which should be specified in terms of Eq. (5-1) and Eq. (5-3). Reasonable physical meaning should be satisfied. That is, when Bond number approaches an infinite value, it means d_p also approaches infinity. When d_p approaches infinity, Eq. (5-1) and Eq. (5-3) should have same S_0. Therefore, coefficient A can be determined as 0.047. So the relationship between irreducible saturation and Bond number was determined as

$$S_0 = 0.047 + 0.022 / N_{Bo} \tag{5-5}$$

The relationship between irreducible saturation and Bond number is shown in Figure 5-9. When the characteristic diameter is small, the Bond number will be small, and surface tension will become the dominant force regardless of the presence of gravity. Thus, smaller particle sizes have a higher irreducible saturation. That means smaller particles are able to hold more moisture before liquid film movement begins. The reason is that smaller particle sizes have a larger specific surface area and there will be a large surface tension force in the fluid contained in a bed of these particles.

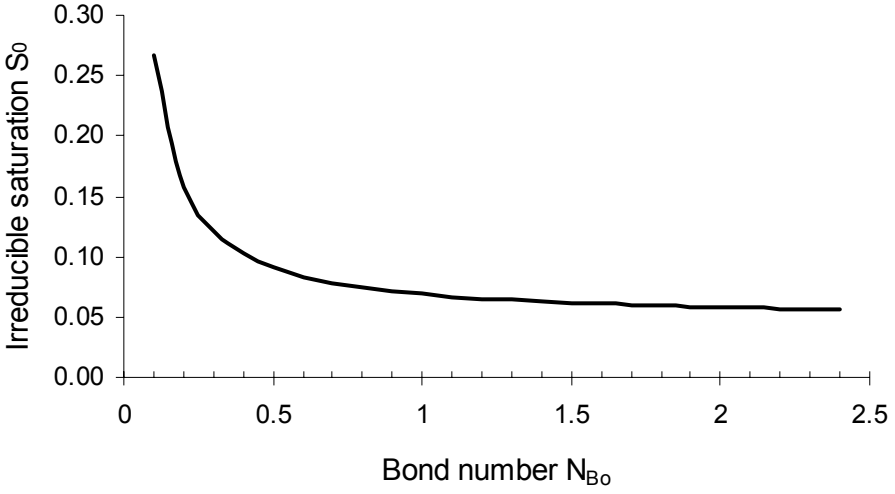

Figure 5-9: Irreducible saturation versus Bond number

5.5 Summary

In this chapter, the irreducible saturation level for different particle size was firstly investigated by performing many experiments with potash beds at various moisture contents with each initial condition close to the irreducible saturation. By comparing experimental data and theoretical/numerical simulation results, the relationship between irreducible saturation and particle size was deduced by curve fitting. It was found that the irreducible saturation is very important and is strong function of particle size. A correlation of irreducible saturation for mixtures of different particle sizes was also developed. This can be used to predict the irreducible saturation of mixtures.

The numerical model that simulates moisture transfer within a potash bed that includes water vapour diffusion and liquid film movement by capillarity and gravity was also validated. Agreement between the experimental data and simulation results is very good and nearly always within the experimental 95% uncertainty bounds of the validation study. The Bond number is introduced to give a brief interpretation about the relationship between irreducible saturation and particle size based on the interaction of capillary and gravity forces.

CHAPTER 6

SUMMARY, CONCLUSIONS AND FUTURE WORK

6.1 Summary

The general purpose of this research is to predict moisture accumulation and movement in potash. Although infiltration, moisture redistribution and drainage of water in potash beds have long been understood to be sensitive to the moisture content, there is little experimental evidence that investigates moisture transport within potash beds by diffusion, capillarity and gravity effects. The first objective in this research was to develop an experimental setup to investigate moisture distribution in a potash bed. The second key objective was to develop and validate a numerical mathematical model that can simulate a one dimensional moisture transfer process in potash under typical storage conditions.

The research carried out can be summarized as follows:

1. A test facility for the investigation of moisture transfer within a potash bed was developed so that moisture redistribution could be accurately measured. Moisture transport experiments were conducted in three layers of an initially stratified potash bed using several different particle size ranges. Each test container was packed with a distinct moisture content into each layer of the bed. Moisture content was measured

gravimetrically. Extensive data was collected for different moisture content combinations, different particle sizes, and various time durations of testing.

2. Some of the most important macroscopic pore structure parameters required for the modeling of moisture transfer within potash bed such as porosity, permeability and specific surface area were investigated through other experimental measurements. The Carman-Kozeny equation with modifications to account for the crystalline shapes of potash was used. The porosity of multi-component particle size mixtures of granular potash was predicted using a correlation based on the porosity and solid volume fraction of each individual particle size component in the mixture. An uncertainty analysis for porosity, permeability and specific surface area was performed to estimate the accuracy of the prediction and show the confidence level for measured results.

3. A theoretical / numerical moisture transfer model considering vapour diffusion, liquid film capillarity and gravity effects was developed to describe the physical processes taking place within a potash bed subject to an initial moisture content or various humidity storage conditions under constant potash bed temperatures. The numerical model was validated by comparison of numerical simulation predictions with experimental data, and the results were presented in terms of spatial and temporal moisture content profiles.

6.2 Conclusions

The above research work led to the following conclusions for the experimental study and numerical simulation of one dimensional moisture transfer within a potash bed.

1. The correlation developed to calculate porosity of binary mixtures of well-shaken or consolidated beds of particles can be used to predict the porosity of multi-component mixtures with different particle size. The modified Carman-Kozeny equation used to account for the crystalline shapes of potash agrees with the experimental data well.

2. The irreducible saturation is very important to the formulation of an accurate unsaturated moisture transport model. It was found that when particle size decreases, the irreducible saturation increases. A correlation of irreducible saturation for mixtures of different particle size was developed for individual particle sizes and for a mixture of particle sizes. This can be used to predict the irreducible saturation of mixtures.

3. The numerical model was validated using experimental data with a small range of uncertainty for selected particle sizes. Vapor diffusion in the dry region and liquid film capillarity and gravity effects in the wet region of a potash bed are the dominant water transfer mechanisms. Agreement between the experimental data and simulation results was within the 95% uncertainty bounds for the validation study for most of the data.

4. This developed numerical model can be used to predict one-dimensional moisture movement within a potash bed by vapour diffusion, liquid film capillarity and gravity effect under an isothermal condition.

5. Simulation results indicate that direct water drainage will occur, for the same initial moisture content, more readily for large particle sizes than for small particles.

6.3 Future Work

Although the current one dimensional numerical model can simulate moisture transfer within potash beds by diffusion, capillarity and gravity effects, it is still at the elementary level for moisture transfer in actual potash storage beds. More research should be done both in experimental and theoretical analyses. In brief, the following recommendations for future work are:

1. A transient dynamic measurement method for moisture content distribution should be developed. The moisture content measured by current gravimetric method is a volume averaged value. If a technique for measuring more data for the spatial moisture distribution were available, it would provide more validation guidance for modeling moisture transfer. A data acquisition system to automatically measure moisture content distribution would be very useful. For example, in terms of the relationship between moisture content and electrical conductivity, developing a set of electrical resistivity

tomography (ERT) measurement system to automatically measure two-dimensional moisture content distribution of potash bed is one possible task.

2. A two-dimensional moisture transport model should be further developed. This would reflect the complex nature of moisture transfer in potash beds in storage sheds.

3. When potash is stored and transported, the ambient temperature often changes. Heat and mass transfer are often coupled in potash storage problems. The mathematical model should be modified to take into account thermal changes, from sensible and latent effects. Potash is stored in different regions with varying temperature conditions, but the numerical model developed in this thesis doesn't consider the influence of temperature. Therefore, developing a transient model to consider both heat and moisture transfer within potash bed is necessary.

REFERENCES

ASHARE Handbook Fundamentals, *American Society of Heating, Refrigerating and Air-Conditioning Engineers, Inc. Atlanta* 1997.

Arinze, E.A., Sokhansanj, S., Besant R.W., Wood, H.C. and Schoenau G.J., "*Experimental & Analytical Moisture Adsorption and Drying Characteristics of Potash Fertilizer Products* ", Powder Handling and Processing, 12(3), pp. 277~287, 2000.

Arinze, E.A., Sokhansanj, S., Besant R.W., Wood, H.C. and Schoenau G.J., "*Effects of Material and Environmental Conditions on Caking and Breakage of Potash Fertilizer Products during Storage, Shipment & Handling*", Powder Handling and Processing, 13(1), pp. 45~54, 2001.

ASME, "*ANSI/ASME PTC 19.1-1985 Part 1, Instruments and Apparatus—Measurement Uncertainty*", ASME, New York, NY 1990.

Cancilla, P., Roy, D., and Rosenblum, F., "*On-line Moisture Determination of Ore Concentrates* ", Bulk Solids Handling, 21(1), pp66~72, 2001.

Carman, P.C. "*Determination of the Specific Surface of Powders. I.",* J. Soc. Chem. Ind. 57, pp. 225~234,1938.

Carman, P.C. "*Determination of the Specific Surface of Powders. II.",* J. Soc. Chem. Ind. 58, pp. 1~7, 1939.

Ceaglske, N.H., and Hoigen, O.A. "*Drying Granular Solids",* Ind. Eng. Chem., 29, pp805~809, 1937.

Dullien, F.A.L. *Porous Media: Fluid Ttransport and Pore Structure*, 2nd ed. Academic Press Inc. Toronto 1992.

Faraji H., Crowe T., Besant R.W., Sokhansanj, S., and Wood H., "*Prediction of Moisture Content of Potash Fertilizer*", *AIC 2002 Meeting, CSAE/SCGR Program*, Paper No.02-307, 2002.

Gao, Q., "*Measurement and Modeling of an Air Wall Jet over Potash Surfaces*", *M.Sc Thesis*, University of Saskatchewan, 2001.

Ghali, K., Jones, B., and Tracy, J., "*Modeling moisture transfer in fabrics*", *Exp. Therm. Fluid Sci.*, 9(3), pp330~336, 1994.

Hansen, L.D., Hoffmann, F. and Strathdee, G., "*Effects of Anticaking Agents on the Thermodynamics and Kinetics of Water Sorption by Potash Fertilizers*", *Powder Technol.*, pp.79~82, 1998.

Kaviany, M., *Principles of Heat Transfer in Porous Media*. 2nd ed. Springer, New York 1995.

Kolphapure, N.H. and Venkatesh, K.V., "*An Unsaturated Flow of Moisture in Porous Hygroscopic Media at Low Moisture Contents"*, *Chem. Eng. Sci.* 52(19), pp3383~3392, 1997.

Malthus T., "*An Essay on the Principle of Population as it Affects the Future Improvement of Society*", Microform, University of Saskatchewan.

Patankar, S.V., *Numerical Heat Transfer and Fluid Flow*, McGrawHill, New York, NY 1980.

Peng S.W., Strathdee, G. and Besant R. W., "*Dissolution Reaction of Potash Fertilizer with Moisture*", *The Can. J. Chem. Eng.*, Vol. 77, pp.1127~1134, 1999.

Peng S.W., Besant R. W. and Strathdee G., "*Heat and Mass Transfer in Granular Potash Fertilizer with a Surface Dissolution Reaction*", The Can. J. Chem. Eng., Vol. 78, pp.1076~1086, 2000.

Puiggali, J.R., Quintard, M., and Whitaker S., "*Drying Granular Porous Media: Gravitational Effects in the Isenthalpic Regime and the Role of Diffusion Models* ", 6(4), pp601~629, 1988.

Pyne, M.T., Strathdee, G., Hansen, L.D., "*Water Vapor Sorption by Potash Fertilizer Studied by a Kinetic Method*", Thermochimica Acta, 273, pp.277~285, 1996.

Thompson, D.C., "Fertilizer Caking and Its Prevention", Proceeding of Fertilizer Society, No. 125, London, UK. 1972.

Walker, G.M., Magee, T.R.A., Holland, C.R., Ahmad, M.N., Fox, J.N., Moffat N.A. and Kells, A.G., "Caking Process in Granular NPK Fertilizer", Ind. Eng. Chem. Res., 37, pp.435~438, 1998.

Whitaker, S. "Simultaneous Heat, Mass and Momentum Transfer in Porous Media: A Theory of Drying", Advances in Drying, Vol.13, pp.119~203, 1977.

Whitaker, S. "Heat and Mass Transfer in Granular Porous Media", Advances in Drying, Vol.1, pp.23~61, 1980.

Yu, A. B.; Standish, N. Porosity calculations of multi-component mixtures of spherical particles. Powder Technol., 52, pp. 233~241. 1987.

Zhou, Q, "Measurement and Simulation of Transient Moisture and Heat Diffusion in a Potash Layer", *M.Sc Thesis*, University of Saskatchewan, 2000.

APPENDIX A

UNCERTAINTY ANALYSIS FOR POROSITY, PERMEABILITY AND SPECIFIC SURFACE AREA

Uncertainty of Porosity

ε_i is the porosity of one sample as determined by a mass (M_i) and volume (V_i) measurement for a potash product of known density (ρ_s).

$$\varepsilon_i = 1 - M_i / \rho_s V_i \tag{A-1}$$

The sample mean for a group of N samples is

$$\bar{\varepsilon} = \frac{1}{N}\sum_{i=1}^{N} \varepsilon_i \tag{A-2}$$

Two types of measurement errors are identified and treated separately throughout uncertainty analysis of porosity measurement. They are precision or random errors, P_ε, and bias or fixed errors, B_ε.

The uncertainty in the mean value of measurement of porosity $\bar{\varepsilon}_i$ is given by

$$U(\bar{\varepsilon}) = \sqrt{B_\varepsilon^2 + P_\varepsilon^2} \tag{A-4}$$

where, B_ε is the bias uncertainty in the measurement of sample weight and volume and the determination of density and is given by

$$B_\varepsilon^2 = \sum_{i=1}^{N}\left(\frac{\partial \varepsilon}{\partial x_i} \cdot B_i\right)^2 \tag{A-5}$$

P_ε is given by

$$P_\varepsilon^2 = \left(t \cdot S_{\bar{N}}\right)^2 = \left(t \cdot S_N / \sqrt{N}\right)^2 \quad \text{(A-6)}$$

where t is the Student t for the 95% confidence level (e.g. t=2.262 when N=10).

The sample standard deviation is calculated as

$$S_N = \sqrt{\frac{1}{N-1}\sum_{i=1}^{N}(\varepsilon_i - \bar{\varepsilon})^2} \quad \text{(A-7)}$$

Table A-1: Bias of measurement parameters for porosity

Bias of volume of container (m^3)	Bias of the mass of bulk potash (g)
1.003×10^{-7}	0.001

For shaken potash with particle size 2.36 mm< d_p < 2.80mm, the $\bar{\varepsilon} = 0.406$,

$B_\varepsilon = 1.63\times10^{-4}$, $S_{\bar{N}} = 7.62\times10^{-7}$, $U(\bar{\varepsilon}) = 0.006$

Uncertainty of Permeability

Permeability is directly measured the using the apparatus shown in Figure 2-4 and is defined by Eq.(2-3).

Air temperature measurement during test was almost constant, and the viscosity of air is 18.1×10^{-6} N·s/m^2 at 22 ºC. The permeability, defined in Eq. (2-3), is a function of pressure difference ΔP, volume flow rate, Q, test container diameter, D, and test sample height, H; i.e. we can write

$$K = K(\Delta P, Q, D, H) \tag{A-8}$$

The uncertainty of permeability can be calculated as

$$U_K = \sqrt{\sum_{i=1}^{n} \theta_i^2 U_{Y_i}^2} = \sqrt{\left(\frac{\partial K}{\partial(\Delta P)}\right)^2 U_{\Delta P}^2 + \left(\frac{\partial K}{\partial Q}\right)^2 U_Q^2 + \left(\frac{\partial K}{\partial D}\right)^2 U_D^2 + \left(\frac{\partial K}{\partial H}\right)^2 U_H^2} \tag{A-9}$$

Table A.2: Uncertainty of measurement parameters for permeability

Parameters	Values
Uncertainty of sample height (m)	0.005
Uncertainty of flow rate (m^3/s)	3.33×10^{-5}
Uncertainty of diameter (m)	0.001
Uncertainty of pressure difference (Pa)	0.154

For shaken potash with particle size 2.36 mm< d_p< 2.80mm, the $U_K = 0.07\times10^{-8}$

Uncertainty of Specific Surface Area

The specific surface area is related to porosity and permeability using the correlation Eq.(2-6), which can be written as

$$A_S = f(\varepsilon, K) \tag{A-10}$$

$$U_{A_S} = \sqrt{\left(\frac{\partial f}{\partial \varepsilon}\right)^2 U_\varepsilon^2 + \left(\frac{\partial f}{\partial K}\right)^2 U_K^2} \tag{A-11}$$

For shaken potash with particle size 2.36<d_p<2.80mm, $U_{\varepsilon} = 0.006$, $U_K = 0.07E-8$, So

$U_{A_S} = 0.17$

APPENDIX B

CONTROL VOLUME FORMULATION FOR DISCRETIZATION OF GOVERNING EQUATIONS AND BOUNDARY CONDITIONS

The discretization equations are derived from the differential governing equations by using control volume formulation method (Patankar, 1980). The typical control volume and solution domain configuration for current one-dimensional case is depicted schematically in Figure B.1 and B.2. For the grid point shown in Figure B.1, uniform grid spacing is used. The fully implicit scheme is employed for the transient terms.

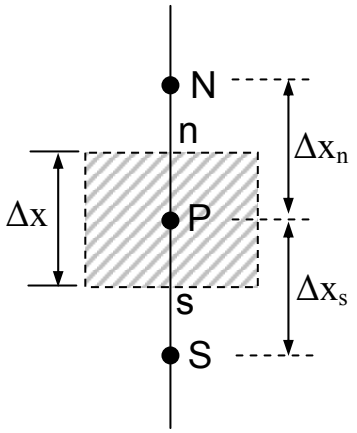

Figure B-1: Geometric schematic of a typical control volume at node P

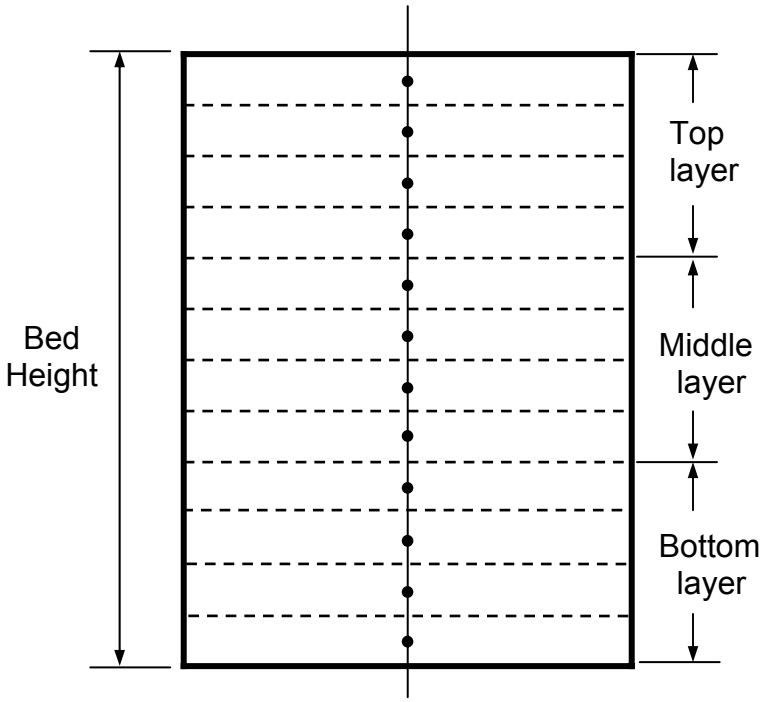

Figure B-2: Schematic of node distribution

in the solution domain of a three-layer potash bed

DISCRETIZATION OF MOISTURE TRANSFER GOVERINING EQUATIONS:

In terms of control volume formulation method, integrate governing equations over the control volume. The detailed deduction process is shown as below.

1. Water Vapour Transfer Equation

The partial differential equation for vapour diffusion in one dimension is rewritten from Eq. (4-10)

$$\frac{\partial(\varepsilon_\gamma \rho_v)}{\partial t} - \dot{m} = \frac{\partial}{\partial x}\left(D_{eff} \frac{\partial \rho_v}{\partial x} \right) \tag{B-1}$$

For the internal nodes, this equation is integrated over the control volume space and over the time period t to Δt

$$\int_s^n \int_t^{t+\Delta t} \frac{\partial(\varepsilon_\gamma \rho_v)}{\partial t} dt dx - \int_t^{t+\Delta t} \int_s^n \dot{m} dx dt = \int_t^{t+\Delta t} \int_s^n \frac{\partial}{\partial x}\left(D_{eff} \frac{\partial \rho_v}{\partial x} \right) dx dt$$

$$(\varepsilon_\gamma \rho_v - \varepsilon_\gamma^0 \rho_v^0)\Delta x - \dot{m}\Delta x \Delta t = \left[\left(D_{eff} \frac{\partial \rho_v}{\partial x} \right)_n - \left(D_{eff} \frac{\partial \rho_v}{\partial x} \right)_s \right] \Delta t$$

where the source term is

$$\dot{m} = S_C + S_P \rho_{vP}$$

The expression for S_C and S_P are dependent on the local relative humidity, Φ and temperature, T. The detailed description of S_C and S_P is presented in the section of source-term linearization part in this appendix.

So,

$$\frac{\left(\varepsilon_\gamma \rho_v - \varepsilon_\gamma^0 \rho_v^0\right)}{\Delta t} = D_{eff_n} \frac{\rho_{vN} - \rho_{vP}}{\Delta x} - D_{eff_s} \frac{\rho_{vP} - \rho_{vS}}{\Delta x} + (S_C + S_P \rho_{vP})\Delta x \tag{B-2}$$

Arrange this equation as the form as $a_P \rho_{vP} = a_N \rho_{vN} + a_S \rho_{vS} + b$, the discretized equation coefficient can be presented as:

$$a_N = \frac{D_{eff_n}}{\Delta x}$$

$$a_S = \frac{D_{eff_s}}{\Delta x}$$

$$a_P = \frac{\varepsilon_\gamma \Delta x}{\Delta t} + a_N + a_S - S_P \Delta x$$

$$b = \frac{\varepsilon_\gamma^0 \rho_{vP}^0 \Delta x}{\Delta t} + S_C \Delta x$$

$$D_{eff_n} = \frac{2D_{effN} D_{effP}}{D_{effN} + D_{effP}}; \quad D_{eff_s} = \frac{2D_{effS} D_{effP}}{D_{effS} + D_{effP}}$$

Similar integration can be used in boundary nodes. The difference between internal nodes and boundary nodes only are: For the top boundary node, a_N=0; for the bottom boundary node, a_S=0.

2. Moisture Transfer Equation by Capillarity and Gravity

The differential equation for liquid moisture transfer is rewritten from Eq. (4-20)

$$\frac{\partial S}{\partial t} = \frac{\rho_\beta g K_\beta^0}{\eta_\beta (1-\varepsilon_\sigma)} \frac{\partial}{\partial x}[(\frac{S-S_0}{1-S_0})^3 (-\frac{\partial h}{\partial S}\frac{\partial S}{\partial x} + 1)] - \frac{\dot{m}}{\varepsilon \rho_\beta} \tag{B-3}$$

Defining $\overline{B}' = \dfrac{\rho_\beta g K_\beta^0}{\eta_\beta (1-\varepsilon_\delta)\cdot(1-S_0)^3}$ and $S' = S - S_0$

Then, Eq.(B-3) becomes

$$B\frac{\partial S'}{\partial t} = \frac{\partial}{\partial x}\left[S'^3 \cdot \left(-\frac{\partial h}{\partial S'} \right) \right] \frac{\partial S'}{\partial x} + \frac{\partial}{\partial x}\left[S'^2 \cdot S' \right] - \frac{\dot{m}}{\varepsilon \rho_\beta A}$$

Defining $K = S'^3 \cdot \left(-\dfrac{\partial h}{\partial S} \right)$, $u = S'^2$, $B = \dfrac{1}{\overline{B}'}$, $S_{source} = -\dfrac{\dot{m}}{\varepsilon \rho_\beta A}$

Then, governing equation can be written as

$$B\frac{\partial S'}{\partial t} = \frac{\partial}{\partial x}\left(K \frac{\partial S'}{\partial x} \right) + \frac{\partial}{\partial x}(uS') + S_{source}$$

Again integrating over one control volume and Δt for an internal node gives

$$\int_s^n \int_t^{t+\Delta t} B\frac{\partial S'}{\partial t} dt dx = \int_t^{t+\Delta t} \int_s^n \frac{\partial}{\partial x}\left(K \frac{\partial S'}{\partial x} \right) dx dt + \int_t^{t+\Delta t} \int_s^n \frac{\partial}{\partial x}(uS') dx dt + \int_t^{t+\Delta t} \int_s^n S_{source} dx dt$$

$$B(S'_P - S'^0_P)\Delta x = \left[\left(K\frac{\partial S'}{\partial x}\right)_n - \left(K\frac{\partial S'}{\partial x}\right)_s\right]\cdot\Delta t + \left[(uS')_n - (uS')_s\right]\cdot\Delta t + S_{source}\Delta x\Delta t$$

$$\frac{B\Delta x}{\Delta t}\left(S'_P - S'^0_P\right) = K_n\frac{S'_N - S'_P}{\Delta x} - K_s\frac{S'_P - S'_S}{\Delta x} + u_n S'_N - u_s S'_P + \frac{S_{source}}{\Delta t} \qquad \text{(B-4)}$$

Arrange this equation as the form as $a_P S'_P = a_N S'_N + a_S S'_S + b$, the discretized equation coefficient can be presented as:

$$a_N = \frac{K_n}{\Delta x} + u_n$$

$$a_S = \frac{K_s}{\Delta x}$$

$$a_P = \frac{B\Delta x}{\Delta t} + a_N + a_S + u_s - u_n$$

$$b = \frac{B\Delta x}{\Delta t}S'^0_P + \frac{S_{source}}{\Delta t}$$

$$K_n = \frac{2K_N K_P}{K_N + K_P}; \quad K_s = \frac{2K_S K_P}{K_S + K_P};$$

$$u_n = \frac{1}{2}(u_N + u_P); \quad u_s = \frac{1}{2}(u_S + u_P)$$

Similar to the boundary node, the difference between internal nodes and boundary nodes only are: For the top boundary node, a_N=0, u_n=0; for the bottom boundary node, a_S=0, u_s=0.

3. Continuity Equation

The continuity of liquid volume flow is rewritten from Eq. (4-11)

$$\frac{\partial \varepsilon_\beta}{\partial t} + \frac{\dot{m}}{\rho_\beta} = 0 \tag{B-5}$$

Integrating for one internal control volume from t to $t + \Delta t$ gives

$$\int_s^n \int_t^{t+\Delta t} \frac{\partial \varepsilon_\beta}{\partial t} dt dx + \int_t^{t+\Delta t} w \int_s^n \frac{\dot{m}}{\rho_\beta} dx dt = 0$$

or

$$\left(\varepsilon_{\beta P} - \varepsilon_{\beta P}^0\right)\Delta x + \frac{\dot{m}}{\rho_\beta}\Delta x \Delta t = 0$$

which becomes

$$\frac{\varepsilon_{\beta P} - \varepsilon_{\beta P}^0}{\Delta t} + \frac{\dot{m}}{\rho_\beta} = 0 \tag{B-6}$$

4. Source-term Linearization for Determination of S_C and S_P

The quantities S_C and S_P arise from the source-term linearization of the form $\dot{m} = S_C + S_P \rho_{vP}$, in terms of the relationship between $\dot{m}$ and relative humidity ϕ as follows.

$$\dot{m} = -\frac{d(\omega)}{d\phi} \cdot \frac{d\phi}{dt} \cdot m_{dry} \tag{B-7}$$

$$\phi = \frac{\rho_v}{\rho_{vsat}} \tag{B-8}$$

$$\frac{\omega}{\omega_m} = \frac{C \cdot \phi}{(1-\phi)\left[1 + (C-1)\phi\right]} \qquad (\phi < 45\%)$$

$$\omega = \frac{1}{d' + e'\phi + f'\phi^2 + g'\phi^3} \qquad (45\% \le \phi < 85\%)$$

The quantities S_C and S_P are given with certain range of relative humidity. That is:

(1) $0 \le \phi < 45\%$

$$S_C = C\omega_m \cdot \left(\frac{1}{(1-\phi)[1+(C-1)\phi]} - \frac{\phi \cdot (C-2-2C\phi+2\phi)}{(1-\phi)^2[1+(C-1)\phi]^2} \right) \cdot \frac{\phi^0}{\Delta t} \cdot \rho_\delta \cdot (1-\varepsilon)$$

$$S_P = -C\omega_m \cdot \left(\frac{1}{(1-\phi)[1+(C-1)\phi]} - \frac{\phi \cdot (C-2-2C\phi+2\phi)}{(1-\phi)^2[1+(C-1)\phi]^2} \right) \cdot \frac{\rho_\delta \cdot (1-\varepsilon)}{\rho_{v\,sat} \cdot \Delta t} \qquad \text{(B-9)}$$

(2) $45\% \le \phi < 85\%$

$$S_C = -\frac{e' + 2f'\phi + 3g'\phi^2}{(d' + e'\phi + f'\phi^2 + g'^3)^2} \cdot \frac{\phi^0 \rho_\delta (1-\varepsilon)}{\Delta t}$$

$$S_P = \frac{e' + 2f'\phi + 3g'\phi^2}{(d' + e'\phi + f'\phi^2 + g'^3)^2} \cdot \frac{\rho_\delta (1-\varepsilon)}{\rho_{v\,sat}\,\Delta t} \qquad \text{(B-10)}$$

APPENDIX C

Numerical Algorithm

The nonlinear coefficients in the differential equations which describe the moisture transport in capillarity and diffusion model present a further challenge to the numerical solution of this set of simultaneous equations. The control volume method (Patankar, 1980), which insures the continuity of mass during transport process, was employed for the spatial discretization of governing equations. To obtain the transient solution, the discretized equations were formulated implicitly in time and simultaneously solved using an iterative procedure within each time step until the required simulation time is reached. The appropriate initial and boundary conditions, and a tri-diagonal solver were used in the calculation process. Figure C-1 shows a flow chart of the calculation process. The detailed solution procedure can be described as follows.

1) Initialize the moisture content profile. Calculate initial saturation, S, distribution from Eq. (4-7) and the initial value of volume fraction of water, $\varepsilon_{\beta,}$ from Eq. (4-22) at initial time level.
2) Based on saturation distribution, determine the area where Eq. (4-6) and (4-10) can be applied.
3) Assume a value of $\dot{m}_b$ at interface point and solve Eq. (4-20) and (4-21) along with all other supplementary equations.

4) Obtain the value of local saturation, *S*, in the region where liquid phase movement equation and vapour diffusion equation is coupled, i.e., region “a” or “a'” shown in Figure 4-4, from the solution of Eq. (4-20) and calculate the local moisture content, ω, based on *S* using Eq.(4-7).

5) Obtain the value of vapour density, $\rho_{v,}$ in region “a” or “a'” from the solution of Eq. (4-21) and calculate the corresponding relative humidity ϕ using Eq.(4-12) and supplementary equations Eq.(4-13), Eq.(4-14) and Eq.(4-15).

6) Check if ω and ϕ satisfy the relationship indicated in isothermal Eq.(4-16) and Eq.(4-17), if necessary, make proper modification on $\dot{m}_b$.

7) Repeat step (3)-(5) till ω and ϕ satisfy relationship shown in Eq.(4-16) or Eq.(4-17) and obtain the solutions of current time step.

8) Repeat step (2)-(6) till desired time step is reached.

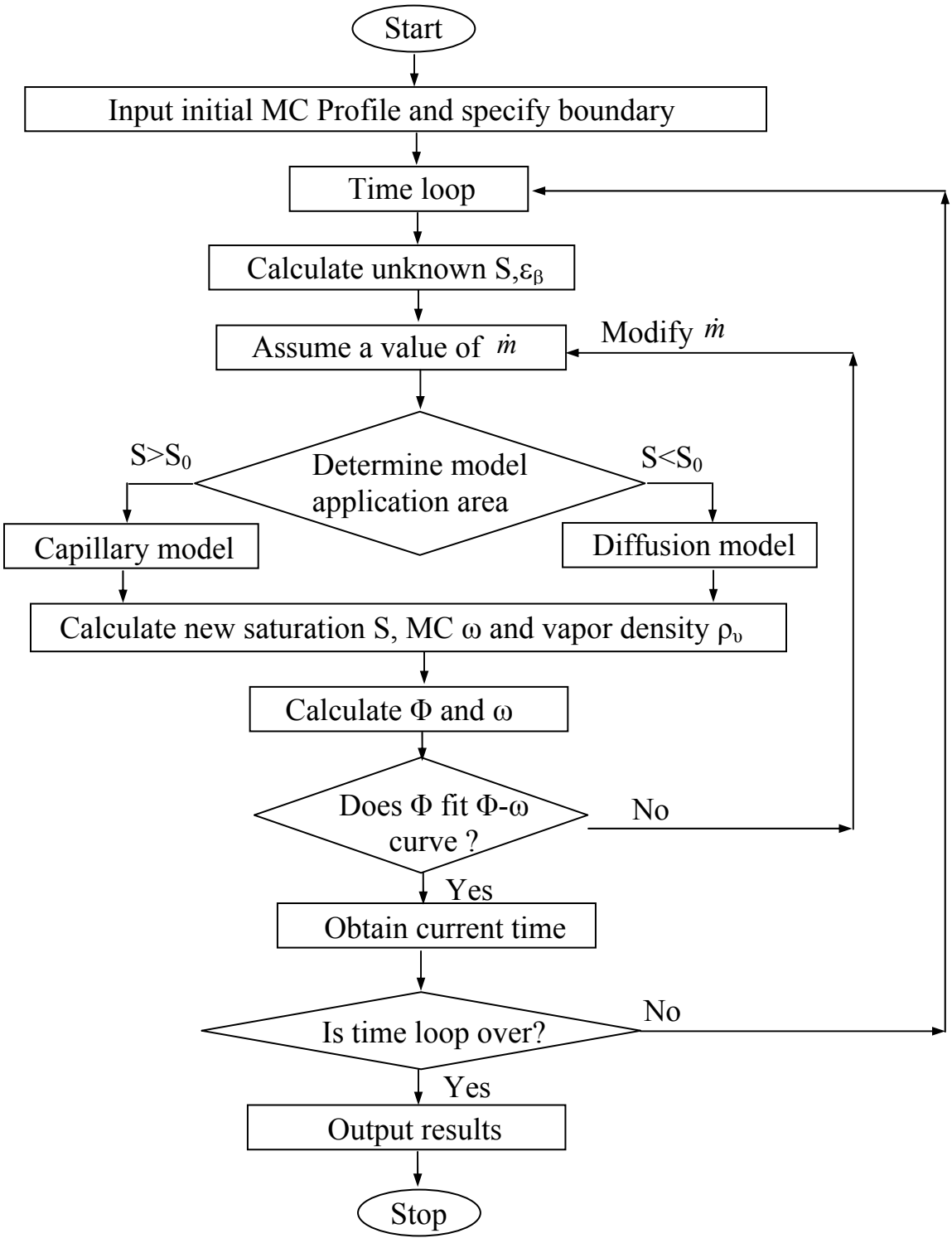

Figure C-1: Schematic of flow chart of the calculation process

APPENDIX D

PROPERTY VALUES USED IN THE NUMERICAL MODEL

Many properties used in the numerical model presented in Chapter 4 are included in this appendix. These properties are either measured from experimental tests or taken from literature. These properties are listed as follows.

τ =1.1 for 2.18mm, τ =1.8 for 0.8mm

ρ_β =997 kg/m^3

ρ_δ =1987 kg/m^3

η_β =1.004E-3 Ns/m^2

ω_m =0.2%

ε = measured value (dependent on particle size, reference to chapter 2)

K_β^0 = measured value (dependent on particle size, reference to chapter 2)

C=1.54

D= 0.26×10^{-4} m^2/s

g = 9.8 m^2/s

R_v = 462 J/(kg·K)

S_0=calculated value (dependent on particle size, reference to chapter 5)

Sl_0 =135 m^{-1} for 2.18 mm, Sl_0 =175 m^{-1} for 0.8 mm

APPENDIX E

MOISTURE TRANSFER EXPERIMENTAL DATA

1. Average Particle Size 2.18mm

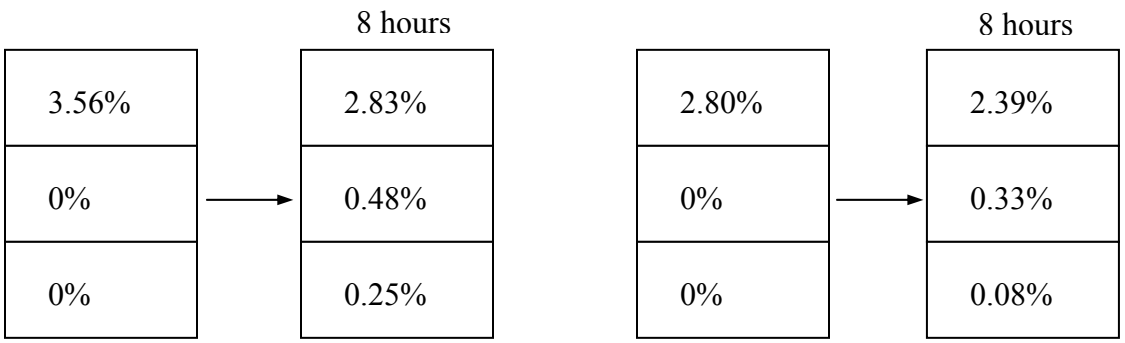

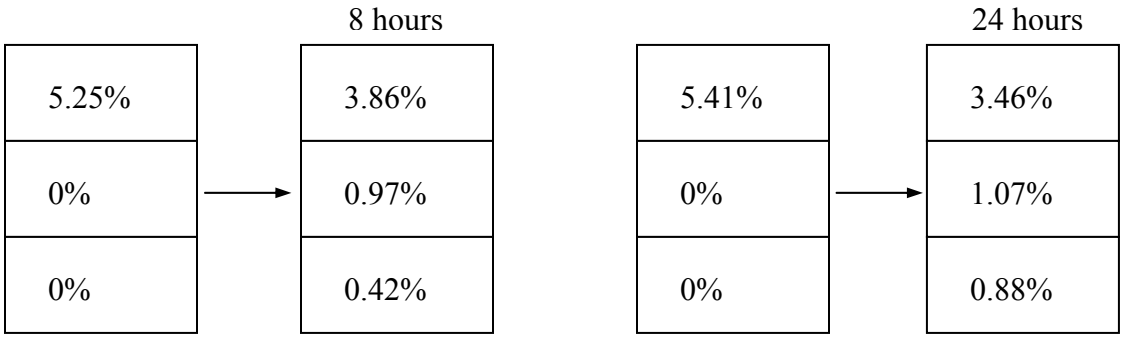

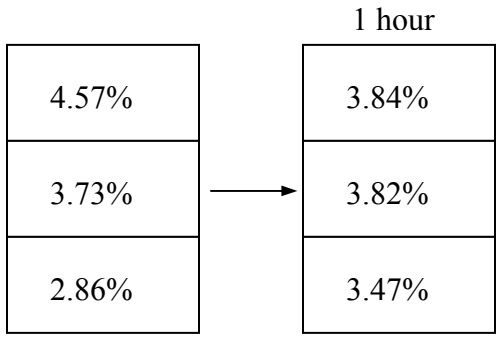
1 hour
4.57%
3.73%
2.86%
3.84%
3.82%
3.47%

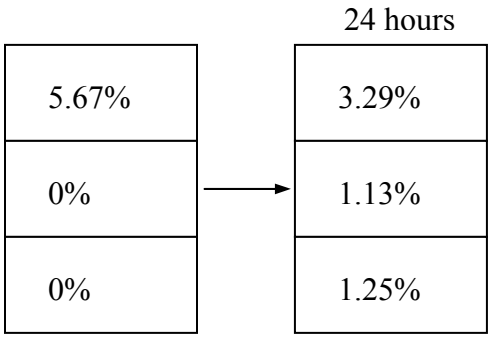
24 hours
5.67%
0%
0%
3.29%
1.13%
1.25%

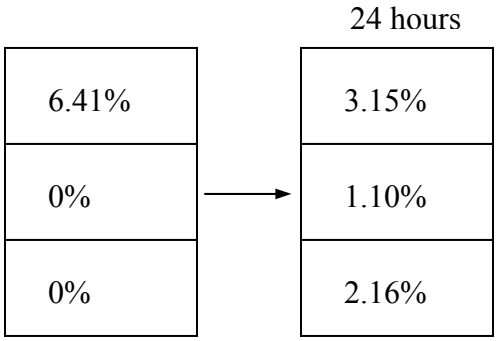
24 hours
6.41%
0%
0%
3.15%
1.10%
2.16%

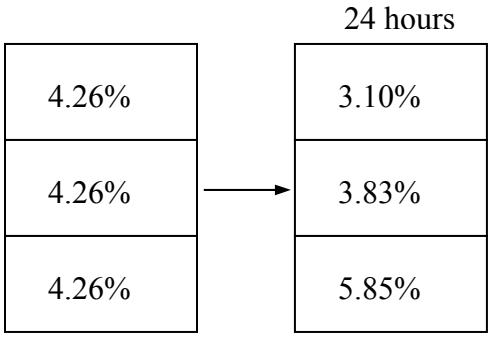
24 hours
4.26%
4.26%
4.26%
3.10%
3.83%
5.85%

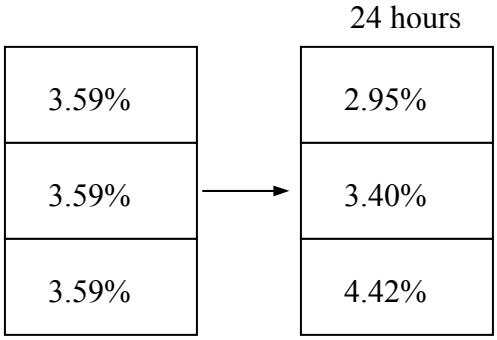
24 hours
3.59%
3.59%
3.59%
2.95%
3.40%
4.42%

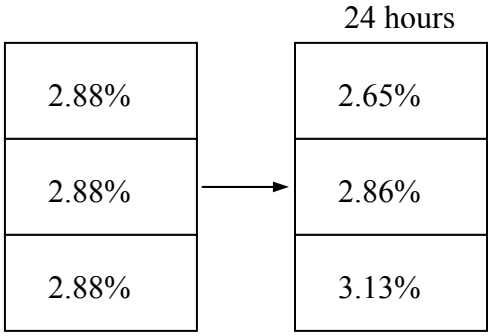
24 hours
2.88%
2.88%
2.88%
2.65%
2.86%
3.13%

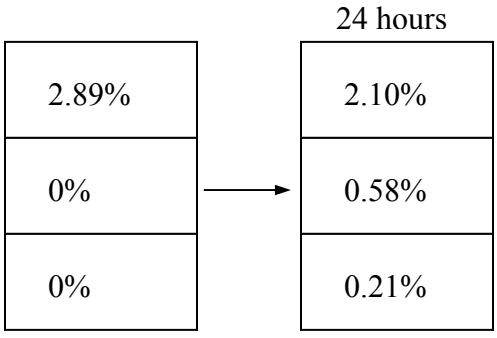
24 hours
2.89%
0%
0%
2.10%
0.58%
0.21%

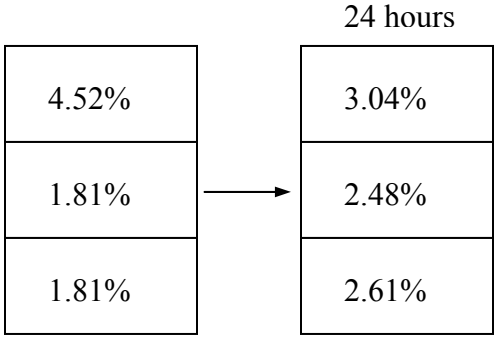
24 hours
4.52%
1.81%
1.81%
3.04%
2.48%
2.61%

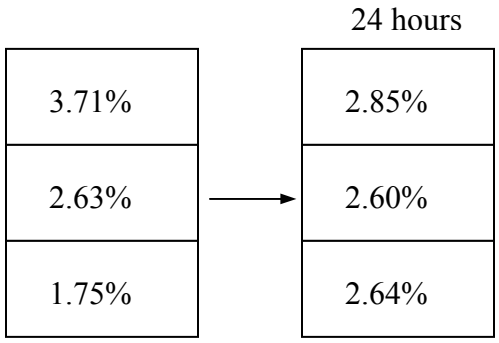

2. Average Particle Size 0.8 mm

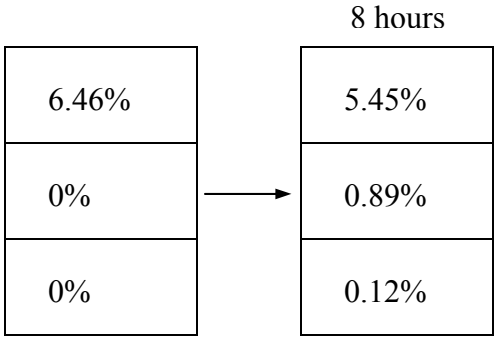

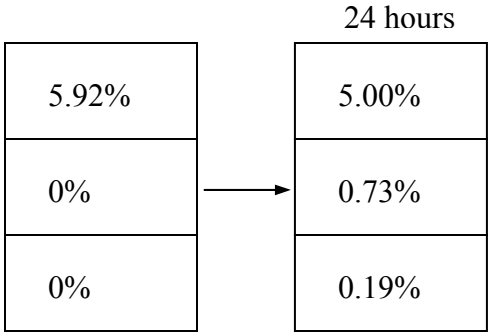

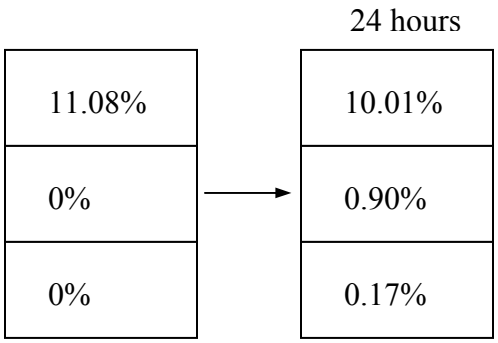

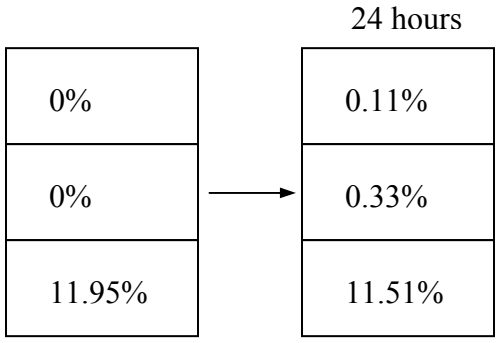

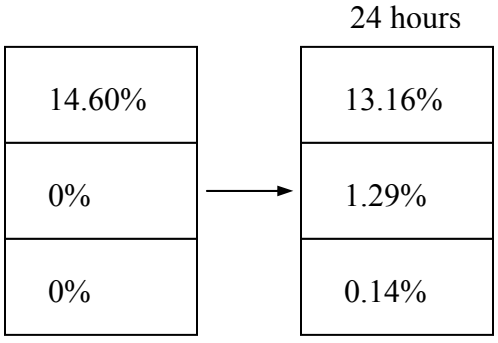

3. Average Particle Size 2.58 mm

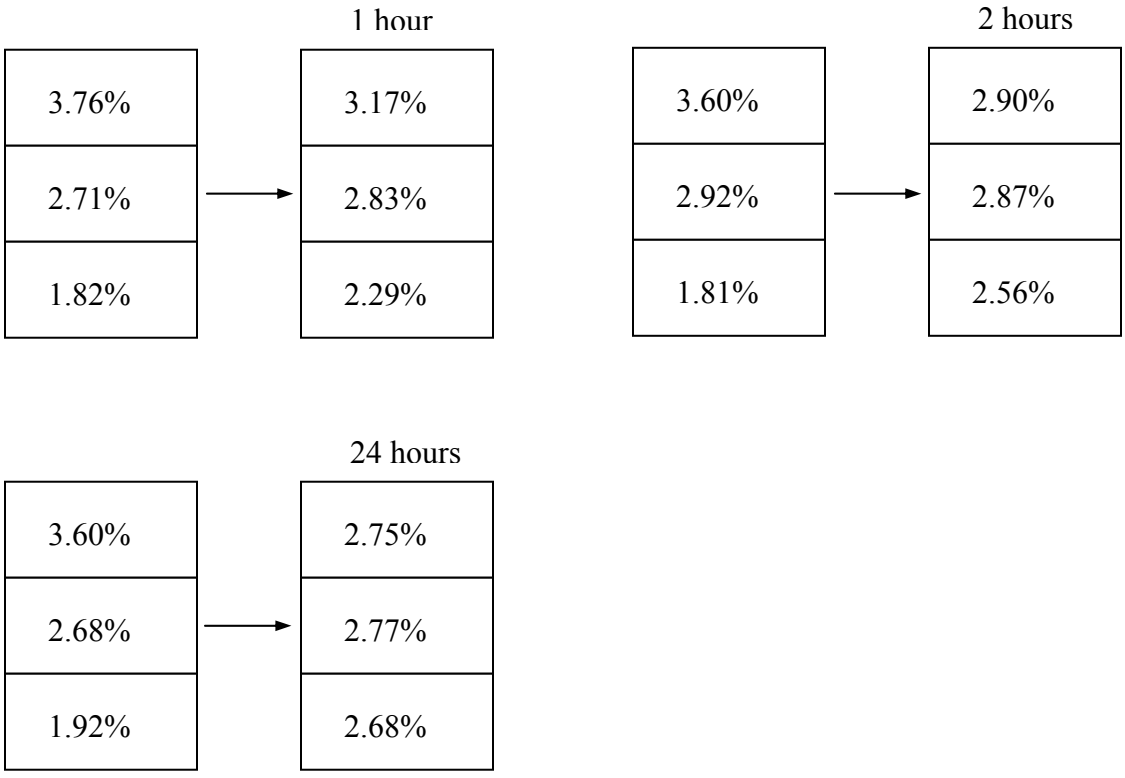

4. Average Particle Size 3.08 mm

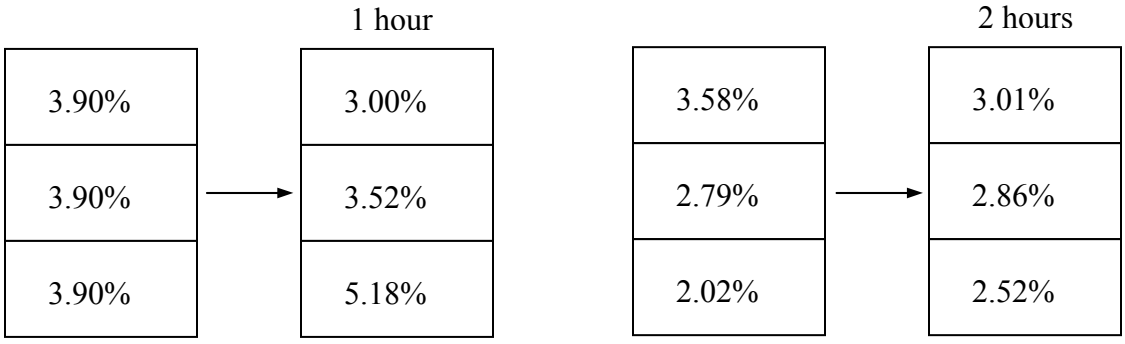

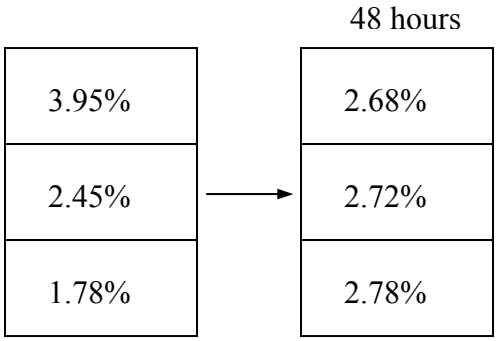

5. Average Particle Size 3.66 mm

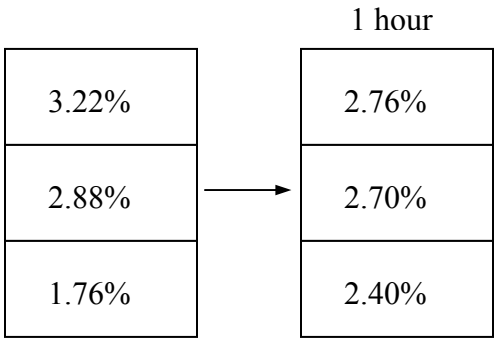

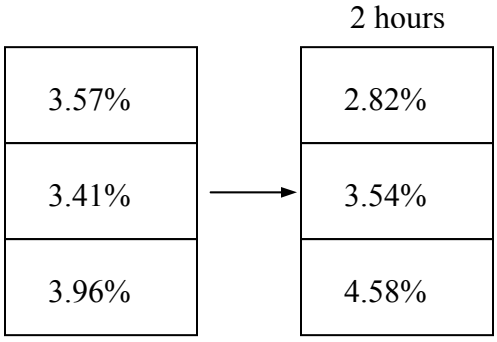

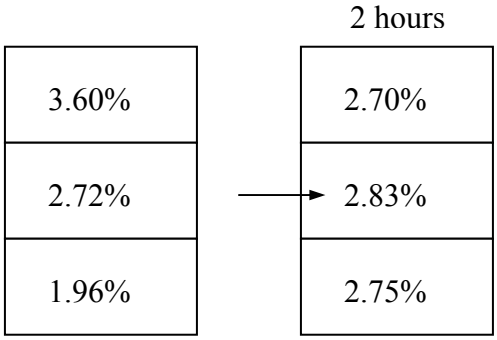

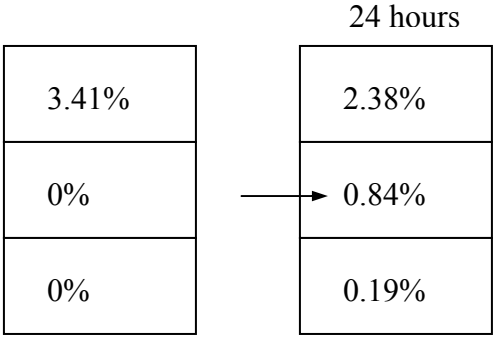

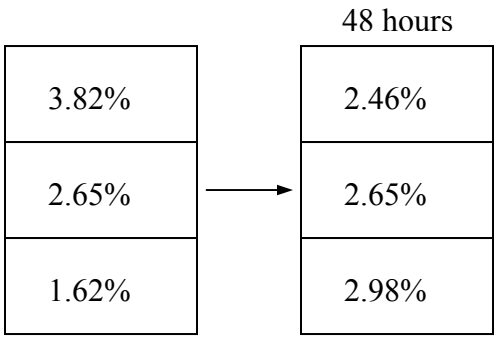

6. Mixture of Particles with 50% dp=2.18mm and 50% dp=3.66mm